https://doi.org/10.5194/gmd-2019-187
Preprint. Discussion started: 25 September 2019

Geoscientific Model Development Discussions

Jena Soil Model: a microbial soil organic carbon model integrated with nitrogen and phosphorus processes

Lin Yu[1], Bernhard Ahrens[1], Thomas Wutzler[1], Marion Schrumpf[1,2], and Sönke Zaehle[1,2]

[1]Max Planck Institute for Biogeochemistry, Hans-Knöll Str. 10, 07745 Jena, Germany
[2]International Max Planck Research School (IMPRS) for Global Biogeochemical Cycles, Jena, Germany

Correspondence: Lin Yu <lyu@bgc-jena.mpg.de>

Abstract. The plant-soil interactions in a changing environment, such as the response of soil organic matter (SOM) decomposition, nutrient release, and plant uptake to elevated CO_2 concentration, is essential to understand the global carbon (C) cycling and predict potential future climate feedbacks. These processes are poorly represented in current terrestrial biosphere models (TBMs) due to the simple linear approach of SOM cycling and the ignorance of variation within the soil profile. While the emerging microbially-explicit soil organic carbon models can better describe C formation and turnover processes, they lack so far a coupling to nutrient cycles. Here we present a new SOM model, JSM (Jena Soil Model), which is microbially-explicit, vertically resolved, and integrated with nitrogen (N) and phosphorus (P) cycle processes. JSM includes a representation of enzyme allocation to different depolymerisation sources based on the microbial adaptation approach, and a representation of nutrient acquisition competition based on the equilibrium chemistry approximation (ECA) approach. We present the model structure and basic features of the model performance against a German beech forest site. The model is capable of reproducing the main SOM stocks, microbial biomass, and their vertical patterns of the soil profile. We further test the model sensitivity to its parameterisation and show that JSM is generally sensitive to the change of microbial stoichiometry and microbial processes.

1 Introduction

There is ample of experimental evidence from both ecosystem monitoring data (Bond-Lamberty et al., 2018; Hou et al., 2018; Jonard et al., 2015) and ecosystem manipulation experiments (Ellsworth et al., 2017; Iversen et al., 2012; McCarthy et al., 2010; Warren et al., 2011) that the effect of environmental changes such as atmospheric CO_2 concentrations, global warming, and continued air pollution on terrestrial ecosystems depends on the constraints imposed by major nutrients such as nitrogen (N) and phosphorus (P). It is therefore fundamental to identify and understand these constraints on the global carbon (C) cycling and storage to predict potential future climate feedbacks (Ciais et al., 2013). There has been a continuous effort to include the N cycle (Thornton et al., 2007; Zaehle and Friend, 2010; Smith et al., 2014) and the P cycle (Wang et al., 2010; Yang et al., 2014; Goll et al., 2017; Thum et al., 2019) to improve the model representation of carbon-nutrient interactions in terrestrial biosphere models (TBMs) over the past decades. However, despite major advances in simulating terrestrial biogeochemistry, these nutrient-enabled TBMs largely fail to reproduce the response to elevated atmospheric CO_2 concentrations as observed in free air CO_2 enrichment (FACE) experiments (Zaehle et al., 2014; Medlyn et al., 2015, 2016). One important shortcoming

https://doi.org/10.5194/gmd-2019-187
Preprint. Discussion started: 25 September 2019

Geoscientific Model Development Discussions

of the current generation of models, is their representation of plant-soil interactions, in particular the response of soil organic matter (SOM) decomposition and nutrient release to altered plant inputs, and therefore plant uptake (Hinsinger et al., 2011; Drake et al., 2011; Zaehle et al., 2014).

Current TBMs largely adopt the CENTURY model (Parton et al., 1988) or comparable model approaches, where soil organic matter is divided into two or three pools with different first-order decomposition rates. In these models, the nutrient mineralisation and immobilization fluxes are dependent on the C transfer efficiency between SOM pools and their prescribed C:N:P stoichiometry. Recent insights of soil science have questioned the CENTURY approach of SOM cycling and pointed out the need and directions for a more mechanistic model representation, such as the representation of substrate limitation of soil microbial growth and nutrient immobilisation as well as the physical stabilization of OM through organo-mineral association (Schmidt et al., 2011). One other important limitation is that most of the current SOM models in TBMs represent the soil as one 'bucket' thus ignoring the strong variance of SOM cycling within the soil profile (Koven et al., 2013). Such a highly empirical representation of SOM cycling, where important processes such as microbial immobilization or rhizosphere deposition are not well represented, brings large uncertainties in future projections of terrestrial C sequestration (Bradford et al., 2016). The inclusions of microbial (enzymatic) dynamics and mineral association in the soil organic carbon (SOC) models has shown the possibilities to represent the SOC responses to warming (Sulman et al., 2018). Moreover, the further inclusion of explicit vertical resolution of biogeochemical processes and transport allows reconciling the SOC depth profile and its ^{14}C profile (Ahrens et al., 2015). Although these new microbial SOC models proved to describe C formation and turnover processes better than the traditional ones, they lack so far a coupling to nutrient cycles.

The main challenge in coupling carbon and nutrient cycles in microbially-explicit models resides in the large stoichiometric imbalances between the microbial decomposer communities, soil micro-organisms, and their resources, plant litter and SOM (Xu et al., 2013; Mooshammer et al., 2014). The microbial community can adapt to these imbalances by adjusting its C:N:P ratios, usually through shifts of community structure such as changes in fungal:bacterial ratios (Rousk and Frey, 2015); or by excreting elements that are in excess through adjusting their elements use efficiencies such as the carbon use efficiency (Manzoni et al., 2012). A more well-known mechanism to adapt to these imbalances is the exudation of extracellular enzymes to release nutrients through hydrolysis (Olander and Vitousek, 2000; Allison and Vitousek, 2005), or to release nutrients by enhancing SOM oxidation, which is known as "rhizosphere priming effect" (Craine et al., 2007; Blagodatskaya and Kuzyakov, 2008). Recent evidence has also shown that soil P availability could regulate the phosphatase synthesis (Fujita et al., 2017) and influence SOM turnover (Lang et al., 2017). Another emerging challenge of representing the nutrient processes in microbially-explicit models is the competition of nutrient uptake between plants and microbes (Dannenmann et al., 2016; Zhu et al., 2017). Particularly for phosphorus, this competition also involves mineral adsorption (Bünemann et al., 2016; Spohn et al., 2018).

Although the above-mentioned processes/phenomena are not yet included neither in current TBMs due to their simple SOM module, nor in current microbial SOC models due to their lack of nutrient cycles, some novel approaches have been proposed in pilot/prototypal models for representing them. One such approach is the microbial adaptation concept, which is applied to represent the adaptation of microbial enzyme allocation to maximize their growth by altering the preferential source of decomposition between plant litter and SOM, as demonstrated by the SEAM model (Wutzler et al., 2017). Another approach

https://doi.org/10.5194/gmd-2019-187
Preprint. Discussion started: 25 September 2019

Geoscientific Model Development Discussions

named equilibrium chemistry approximation (ECA), is proposed to simulate the competition of substrate uptake kinetics in complex networks by taking account the impact of one uptake kinetic on other substrates (Tang and Riley, 2013), and has been applied to resolve mineral nutrient sinks (plant-microbe uptake or mineral adsorption) competition in prototype model studies (Zhu et al., 2016, 2017).

In this study, we present the structure and basic features of a new microbially-explicit, vertically resolved SOM model integrated with N and P cycle processes, the Jena Soil Model (JSM). We test and evaluate alternative hypotheses on the competition of microbial, plant, and mineral nutrient sinks (uptake or mineral sorption), and the effect of nutrient availability on the preferential decomposition of either nutrient poor or rich organic matter using observed profiles of soil carbon, nitrogen and phosphorus in a temperate beech forest stand. Additionally, we provide an assessment of the model's sensitivity to its parameterisation and the associated uncertainty to help understanding these effects.

2 Material and methods

2.1 Model description

The Jena Soil Model (JSM) is a soil biogeochemical model and was built on the backbone of the vertically explicit carbon-only soil organic carbon model COMISSION (Ahrens et al., 2015). The COMISSION model was further developed compared to Ahrens et al. (2015) by introducing a scalable maximum sorption capacity based on soil texture for DOC and microbial residues (Sect. 5) and by introducing temperature and moisture rate modifiers for the microbially mediated processes and sorption (Sect. 5). We will investigate in a separate study how a maximum sorption capacity for mineral-associated organic carbon contributes to observed patterns of SOC radiocarbon ages. A schematic overview of the JSM model is shown in Fig. 1, the mathematical description of the processes is given in Appendix A. The model is integrated into the modelling framework of the QUINCY TBM (Thum et al., 2019) and can be applied as a stand-alone soil module or coupled to the representation of vegetation and surface processes. In this study, we apply JSM as stand-alone model. JSM does not describe the energy and water processes at the atmosphere-soil interface or in the soil profile, nor does JSM simulate the production of litter fall. Model inputs (soil temperature, moisture and water fluxes, as well as the litter fall data as the model inputs) are derived from the QUINCY model.

JSM describes the formation and turnover of SOM along a vertical soil profile, which is explicitly represented with exponentially increasing layer thickness as soil depth increases (Fig. 1). The biogeochemical processes and pools of C, N, and P are represented in each layer. Vertical transport of biogeochemical pools between adjacent layers due to percolation and bioturbation is also modelled. To reflect the development of an organic layer, the model also includes an extra advective transport term which accounts for the upward/downward shift of the soil surface when the surface SOM accumulates/diminishes.

SOM is represented as pools of soluable, polymeric, and woody litter, as well as dissolved organic matter (DOM), mineral-associated DOM, living microbial biomass, microbial residue (necromass), and mineral-associated microbial residue, each of which contains organic forms of C, N and P. The flow of organic N and P follows the pathways of C, with extra nutrient-specific processes, such as mineralisation and plant uptake to link organic matter turnover with inorganic nutrient cycles. Microbial biomass is assumed to maintain a fixed stoichiometry in the model, requiring the microbial synthesis of C, N and P

https://doi.org/10.5194/gmd-2019-187
Preprint. Discussion started: 25 September 2019

Geoscientific Model Development Discussions

to fulfill the C:N:P ratio of the microbial biomass pool. The stoichiometry of all other SOM pools depends on the C:N:P ratios of influx and efflux, and these fluxes all retain the stoichiometry of their sourcing pools, unless the formation processes involve respiration. In addition, when microbes decay, nutrients are preferably recycled to DOM pool due to the low C-to-nutrient ratio in the cyctoplasma, as proposed by Schimel and Weintraub (2003). The inorganic pools of N and P include soluble inorganic ammonium (referred as NH_4), nitrate (refered as NO_3), soluble inorganic phosphate (referred as PO_4), as well as adsorbed PO_4, absorbed PO_4, occluded PO_4 and primary PO_4. The inorganic P cycle follows the QUINCY model (Thum et al., 2019), with modifications due to microbial interactions.

Enzymes are not explicitly modelled in JSM, but are described implicitly to regulate processes such as depolymerisation and nutrient acquisition. For enzyme allocation within depolymerisation process, we extended the microbial adaptation approach of the SEAM model (Wutzler et al., 2017) by including P and vertical explicitness and assuming a steady state of enzyme production, which means enzyme level is always proportional to the microbial biomass. The fractions of enzyme allocated to different depolymerisation sources (litter and microbial residue) are dynamically modelled to maximize the release of the most limiting elements of microbes (See Sect.5). For nutrient acquisition of plant, microbes and soil adsorption sites (only for phosphate), the potential rates are calculated based on the respective enzyme richness, half-saturation level of enzymes, and the impacts from other competitors following the ECA approach (See Sect.5).

2.2 Site and data

The Vessertal (VES) site is a mature beech (*Fagus sylvatica*) forest stand and an average tree age of more than 120 years, located in the German central uplands (Thuringian Forest mountain range). The site has an intermediate elevation of 810 m a.s.l with high annual precipitation of 1200 mm and a mean annual temperature of 5.5 °C (Lang et al., 2017). It is one of the Level II intensive monitoring plots of the Pan-European International Co-operative Program on assessment and monitoring of air pollution effects on forests (ICP Forests). The VES site has also been selected as one of the main study sites in the DFG funded priority programme 1685 'Ecosystem Nutrition: Forest Strategies for limited Phosphorus Resources' since 2013.

The soil was classified as Hyperdystric skeletic chromic cambisol (WRB, 2015) with a loam topsoil and sandy loam subsoil and is overlain by Moder organic layer. The current soil was developed on Trachyandesite, and the development started at the end of the last ice age, 10–12,000 years ago (Lang et al., 2017).

The soil contains 19 kg/m^2 C, 1.1 kg/m^2 N, and 464 g/m^2 P up to 1 m soil depth including the forest floor (Lang et al., 2017). The C content of SOM decreases from 510 g/kg in the forest floor to 126 g/kg in the A horizon and 5.9 g/kg at 1 m depth. The C:N ratio of SOM slightly decreases from ca. 30 in the forest floor to ca. 20 at 1 m depth, while the decrease of the C:P ratio is stronger—from ca. 2500 in the forest floor to ca. 300 at 1 m depth. The organic fraction of total P also decreases from two thirds in the organic layer to ca. 10 % at 1 m depth. The microbial C content decreases from more than 2000 $\mu g/g$ C in the forest floor (Zederer et al., 2017) to 764 $\mu g/g$ C in the top mineral soil (Bergkemper et al., 2016). The microbes have a C:N ratio of 13 and a very low C:P ratio of 10.3 (Lang et al., 2017).

https://doi.org/10.5194/gmd-2019-187
Preprint. Discussion started: 25 September 2019

Geoscientific Model Development Discussions

2.3 Model protocol, model experiments, and sensitivity analysis

Model protocol and calibration

The soil texture profile for both QUINCY and JSM simulations was taken from the observations at the VES site. The mineral-associated DOM and residue pools were initialised based on Eq.S7, using observed soil texture and mineral soil density, and assuming that soil surface sorption sites are less occupied as soil depth increases. The vertical profile of the other SOM pools was initialised with a default C content for each pool in the first layer and assumed to decrease with soil depth in proportion to the fine root profile (Jackson et al., 1996), except the woody litter which is only initialised in the first layer. The initialisation C content in first layer for soluable litter, polymeric litter, woody litter, DOM, microbes and microbial residue are 291, 2914, 1000, 2.4, 73.2, and 203 $\mathrm{g/m^3}$ C, respectively. The N and P content of the SOM pools were initialised with stoichiometry of different pools: for litter pools, we adapted the litter stoichiometry from the QUINCY model (Thum et al., 2019); for microbes and microbial residues, we used the measured microbial stoichiometry (Bergkemper et al., 2016); for other SOM pools, we used the measured average SOM stoichiometry of the 1 m soil profile (Lang et al., 2017). The soil inorganic P pools were initialised using the soil P data-set by Yang et al. (2013), corrected with the current total inorganic P from field measurements and extrapolated to the whole soil profile following the approach used in the QUINCY model (Thum et al., 2019). The organic matter material density and mineral soil density were solved using the Federer equation (Federer et al., 1993) with the field data of SOM content and bulk density. [1]

We simulated the VES site for 200 years using JSM, repeating 30 years of soil forcing (half-hourly soil temperature, soil moisture, vertical water fluxes, and vertically resolved litter fall) simulated by the QUINCY model for the VES site. To mimic the history of $^{14}\mathrm{C}$ input, we assumed increased litter $^{14}\mathrm{C}$ content for the final 60 years before the end of the simulation, matching the observed $^{14}\mathrm{CO_2}$ atmospheric pulse. We tested different simulation lengths (50, 200, 1000, 5000, and 10000 years) and found out that simulated SOM profile changes slowly after 200 years but the soil inorganic P pools changes gradually as the simulation time increases (data not shown). Therefore, we chose to compare the present-day soil profile observations with the simulated profiles from the 200-year simulations, which best fit the time of the soil inorganic P pool initialisation (1850, as indicated in Yang et al. (2013)). All the other presented results are also based on the 200-year simulations, and the results of long-term simulations (1000y and 5000y) can be found in the supplementary materials.

The calibration processes consisted of two main steps: in the first step we match the model results with the measured SOC profile, mainly by calibrating the depolymerisation, OM sorption, and litter turnover processes; in the second step, we match the model results with the measured soil organic P profile by calibrating the microbial growth & decay, nutrient acquisition, and soil inorganic P cycling. Other observed soil profiles were used as extra criteria to select parameterisation but not particularly used to calibrate the model.

Model experiments

[1] Solved by Microsoft Excel, using the Generalized Reduced Gradient nonlinear optimization method with algorithm developed by Leon Lasdon, University of Texas at Austin, and Alan Waren, Cleveland State University, and enhanced by Frontline Systems, Inc.

https://doi.org/10.5194/gmd-2019-187
Preprint. Discussion started: 25 September 2019

Geoscientific Model Development Discussions

To further test the effects of different model features, we implemented several model experiments, including: a *SEAM-off* scenario where the enzyme allocation to polymeric litter and microbial residue are both fixed to 50 % (Eq.1b), and a *ECA-off* scenario where the ECA-based plant and microbial uptake of inorganic N & P and soil adsorption of phosphate was switched off, and replaced by a demand-based microbial uptake of inorganic N & P and ignored phosphorus adsorption flux (Eq.1c). All the model experiments use the same parameterisation from the calibrated model with full model features, which is denoted as the *Base Scenario* in this study. The differences between *Base Scenario* and *SEAM-off* & *ECA-off* are listed below,

$$
\begin{aligned}
&Base\ Scenario: \\
&\qquad Enz_{frac}^{poly} \& \ Enz_{frac}^{res} \text{ calculated as Eq.S15} \\
&\qquad U_{X,y}^{*} \text{ for microbes, plant, and adsorption calculated as Eq.S23} \qquad (1a) \\
&SEAM-off\ Scenario: \\
&\qquad Enz_{frac}^{poly} = Enz_{frac}^{res} = 0.5 \qquad (1b) \\
&ECA-off\ Scenario: \\
&\qquad U_{X,plant}^{*} = f(T_{soil},\Theta) v_{max,plant}^{X} C_{fine\_root}[X](K_{m1}^{upt} + \frac{1}{K_{m2}^{upt}+[X]}) \\
&\qquad U_{X,mic}^{*} = F_{mic,X}^{demand} \\
&\qquad U_{P,adsorp}^{*} = 0 \qquad (1c)
\end{aligned}
$$

The plant uptake of inorganic N or P ($U_{X,plant}^{*}$) in the ECA-off scenario (Eq.1c) uses the same equation and parameters from the QUINCY model (Thum et al., 2019). Other model experiments to demonstrate the effects of microbial stoichiometry and simulation time can be found in the supplementary material.

Model sensitivity

We further test the sensitivity of JSM to its parameterisation using a hierarchical latin hypercube design (LHS, Saltelli et al., 2000; Zaehle et al., 2005). We select 28 parameters from the calibration (TabS4) and varied each parameter between 80% and 120% of the Base Scenario values given in the Tab.S3, drawn with LHS sampling from a uniform distribution to form a set of 1000 LHS samples, which are used for the model sensitivity and uncertainty analysis presented in this paper. We evaluate the model output from these simulations in terms of main biogeochemical fluxes, such as respiration, net N & P mineralisation, microbial uptake of inorganic N & P, N & P losses, and P biomineralisation, and main SOM pools (up to 1 m depth), such as total C, N, and P in SOM, total soil inorganic P, and microbial C, N, and P. We measure parameter importance as the rank-transformed partial correlation coefficient (RPCC) to account for potential non-linearities in the relationship between parameters and model output (Saltelli et al., 2000; Zaehle et al., 2005).

https://doi.org/10.5194/gmd-2019-187
Preprint. Discussion started: 25 September 2019


Geoscientific Model Development Discussions

3 Results

3.1 Simulated SOM stocks and fluxes at the study site

In this study, we tested different simulation lengths of JSM and found out that the simulated SOM profiles, including the SOC, C:N and C:P ratios of SOM, microbial C, N, and P content, and bulk density, don't change much with time (Fig.S1). Therefore in this study, we focus on the stable state at the end of the 200-year simulations and refer to it as a "quasi-equilibrium state" since slow changes are still occurring, especially with soil inorganic P pools and with SOM in deeper soils (Fig.S3 and S4).

We first compare the simulated profiles with the *in situ* observations (Fig.2). The modelled results agree well with the observed stock sizes and vertical patterns, and indicate that the stocks of C, N, and P in SOM have smaller temporal variations than the stocks in microbes at the quasi-equilibrium state (Fig.2a to 2c), due to the strong seasonal variations in the microbial biomass. We also find a stronger variation in the simulated organic P to inorganic P (Po-to-Pi) ratio (Fig.2d) than for organic P and inorganic P stocks separately (data not shown), inferring that the seasonal dynamics of microbes also impose a seasonal pattern to P immobilisation (from Pi to Po) and mineralisation (from Po to Pi).

The distribution of total OM at each depth across OM-pools and their radiocarbon content in the simulations are displayed in Fig.7. The first layer (0cm, O-A horizon) is dominated by the plant litter and microbial component (living/dead microbes), while the microbial component decreases strongly from ca. 40% at 0cm to almost none at 50cm soil depth, the litter component still consists ca. 10% of the total SOC at 1m soil depth. The mineral-associated carbon (MOC) component switches from a minor component in the O-A horizon (ca. 20%) to the dominant component (ca. 90% at 1m) in the deeper soil.

The simulated radiocarbon ($\Delta^{14}C$) profile agrees with the observations in so far that the $\Delta^{14}C$ values increases within the O horizon and starts decreasing with soil depth from mineral soil, i.e. A horizon (Fig.S1e). This pattern indicates the 'bomb pulse' of $\Delta^{14}C$ signal significantly affect the apparent ^{14}C age in the organic layer due to the strong litter interactions and the impacts decrease with soil depth due to the slow turnover in deeper soil. Our simulations further indicate that such a vertical pattern is caused by the MOC and microbial components, while the litter component shows a general increase of radiocarbon percentage with increasing soil depth (Fig.7). Although the Base Scenario does not reproduce the measured radiocarbon profile but only the vertical pattern, we do see a much better fit with measured radiocarbon profile and an increase of soil ^{14}C age, which are driven by MOC as the simulation length increases (Fig.S1e and Fig.S3).

The simulated biogeochemical fluxes show a strong seasonal and vertical pattern (Fig.3 and Fig.4), in which the flux rates in summer and in the top layer are generally higher than those in winter and in the subsoil, respectively. However, the microbial uptake of inorganic N shows a different seasonal pattern where the rate is lowest in August and September (Fig.4c). This pattern is actually supported by the seasonal pattern of net N mineralisation flux where the peak is found in August and September (Fig.3b). This indicates that the organic N in DOM is most abundant for microbial growth during August and September, which leads to a strong reduction in the microbial inorganic N uptake and increase in the net N mineralisation. To the contrast, the organic P in DOM is most scarce during August and September, and it leads to a negative net P mineralisation and an increase of microbial inorganic P uptake (Fig.3d and Fig.4a). While the vertical pattern of plant N uptake follows that of the root

https://doi.org/10.5194/gmd-2019-187
Preprint. Discussion started: 25 September 2019


Geoscientific Model Development Discussions

distribution (Jackson et al., 1996), the plant P uptake is lower in the organic layer than the topsoil due to the strong competition from microbes in the organic layer (Fig.4 and Fig.5).

In general, the SEAM-Off scenario does not differ much from the Base Scenario with regard to the main soil stocks and biogeochemical fluxes (Fig.2 and Fig.3), but the ECA-Off scenario produces a lower microbial biomass and a lower Po-to-Pi ratio in the organic layer and top soils. The total SOC seems not to be influenced in both scenarios, but the composition of SOC and the radiocarbon profile are all altered (Fig.7).

3.2 Model features: nutrient acquisition competition and enzyme allocation

We present the microbial and plant uptake rates of inorganic PO_4 and the competition between phosphate adsorption, microbial and plant uptake of inorganic P at three different depths (Fig.5), as well as the seasonal and vertical uptakes of inorganic N and P for both microbes and plant (Fig.4). The simulations show that microbes outcompete roots for inorganic P (TW: in JSM) in all the chosen depths, but the relative competitiveness of roots to take up phosphate increases with soil depth. In other word, the plant P uptake rate decreases less strongly than the microbial P uptake with increasing soil depth. The phosphate adsorption rate, in contrast, increases strongly with increasing soil depth and outcompetes biological processes (plant and microbial uptake) in the deeper soil. The relative competitiveness of phosphate adsorption also shows a strong decrease in summer in the top soil, due to the high biological activities in warm months (Fig.5B). For the competition of inorganic N, plants outcompete microbes along the whole soil profile and through the whole seasons, especially in summer when microbes assimilate N mainly from DOM (Fig.4c and d).

Turning off the model feature of the nutrient acquisition competition, i.e. ECA-Off scenario, leads to a noticeably lower microbial biomass and Po-to-Pi ratio in the top soil (Fig.2). This is caused by the concurrent changes in the inorganic P uptake of microbes and plant, especially in the top layer where plants take up more inorganic P than the Base Scenario (Fig.4) due to less competition from microbes. We also observe different spatial and temporal variation of fluxes in the ECA-Off scenario from the other two scenarios. For example, the seasonal variation of fluxes is notably lower in the ECA-Off scenario. The decrease of P flux rates with soil depth seems less strong in the ECA-Off scenario, but the decrease of net N mineralisation with depth is more significant (Fig.3). This difference is due to the fact that the geophysical processes, such as adsorption and absorption, play a much more important role in the soil P cycle than in the N cycle and they have a quite different seasonal and vertical pattern from the biochemical processes, such as mineralisation.

The modelled enzyme allocation for depolymerisation process is presented in Fig.6. In the figure, we compare the actual enzyme allocation curve of polymeric litter with three potential allocation curves, which represent the cases when microbes only want to maximize C, N, or P release from depolymerisation. The modelled fractions of actual enzyme allocation to polymeric litter are all well below 50% for the whole soil profile, indicating that polymeric litter is the less preferred than microbial residues for depolymerisation in the soil, particularly in the very deep soil where no roots are presented and microbes would only produce enzyme to depolymerise microbial residues. The simulated curve of actual allocation overlaps with the curve of potential allocation to maximize P release, indicating that the depolymerisation process is solely driven by the P demand. This indication explains why microbial residues are preferred over polymeric litter, since the C:P ratio of microbial

https://doi.org/10.5194/gmd-2019-187
Preprint. Discussion started: 25 September 2019

Geoscientific Model Development Discussions

residues is much higher than that of the polymeric litter (data not shown). Despite the very different enzyme allocation fractions shown in Fig.6, most of the modelled stocks and fluxes are not significantly influenced when the enzyme allocation is turned off (Fig.2 and 3). More profound differences are seen in the SOC composition and the radiocarbon profile that there are less litter and more SOC in the SEAM-Off scenario than in the Base Scenario, resulting a systematic difference in the radiocarbon profile.

3.3 Model sensitivity and uncertainties

The inner-quartile range of the outputs (Fig.9) from the model sensitivity study reveals that all the outputs are well centered around the results of the parameterisation of the Base Scenario (Tab.S4). In general, the soil stocks are more stable than the microbial pools and biogeochemical fluxes, whereas the mineralisation of N is surprisingly resistant and the microbial uptake of inorganic N is very sensitive to the parameter changes. The mineralisation of N in JSM is mainly driven by the C:N ratio of the DOM, which is quite stable due to the similar C:N ratios of plant litter, microbes, and microbial residues. The very sensitive response of microbial uptake of inorganic N is because microbes have high affinity (low $K_{m,mic}$ value) transporters for N uptake (Kuzyakov and Xu, 2013) and is sensitive to the concentration change of NH_4. The relative partial correlation coefficient (RPCC) of parameters with outputs (Tab.2) also demonstrates that the C and N content in SOM and the C, N fluxes respond more to the changes of C processes, i.e. depolymerisation, OM sorption, and litter partitioning, while the microbial dynamics and the P fluxes are more prone to the changes of microbial and nutrient processes, such as maximum biomineralisation rate ($v_{max,biomin}$) and recycling of P during microbial decay ($\eta^{P}_{res\rightarrow dom}$). Overall, most of the selected outputs are strongly influenced by the microbial stoichiometry. The five most influencing parameters in JSM are microbial C:N ratio ($\chi^{C:N}_{mic}$), microbial N:P ratio ($\chi^{N:P}_{mic}$), microbial mortality rate (τ_{mic}), fraction of soluble litter C transformed into DOM ($\eta_{C,sol\rightarrow dom}$), and fraction of P recycled from res to dom during microbial decay ($\eta^{P}_{res\rightarrow dom}$).

4 Discussions

4.1 Features of nutrient cycling

Soil stoichiometry

The JSM is able to reproduce the main soil stocks of C, N, and P, microbial biomass, and soil bulk density, as well as their vertical patterns along the soil profile in a German beech forest site. The observed C:N ratio (19.5) and C:P ratio (348) in the first model layer, O-A horizon, fit well within the ranges of the reported soil stoichiometry of temperate broadleaf forest (Xu et al., 2013), and there is a much stronger decreasing trend of C:P ratio than C:N ratio as soil depth increases, indicating that the organic P in SOM is "decoupled" from the CN cycles (Yang and Post, 2011; Tipping et al., 2016).

This decoupling effect of soil P cycle is represented by the biomineralisation process in TBMs, but the vertical decoupling of C:N:P stoichiometry was poorly reproduced (Fig.S5) even when the microbial biomass is explicitly represented (Yu et al.,

https://doi.org/10.5194/gmd-2019-187
Preprint. Discussion started: 25 September 2019


Geoscientific Model Development Discussions

2018). Our study indicates that the decrease of C:N ratio is mainly due to the SOC composition shift with soil depth (Fig.7), that said the fraction of nutrient-poor litter component decreases and the fraction of nutrient-rich MOC component increases.

However, for the decrease of C:P ratio, the model simulations indicate that the change of microbial nutrient recycling scheme with depth might play a bigger role than the SOC component shift. To account for the different stoichiometry of cell walls and plasma of microbes in JSM, we introduce the microbial nutrient recycling parameter ($\eta^{X}_{res\rightarrow dom}$, X for N or P) that assigns microbial residues with a higher C:N:P ratio than DOM when microbes decay. Due to the fact that JSM currently does not distinguish microbial guilds, the microbial nutrient recycling parameter also mimics different stoichiometry of microbial guilds, such as bacteria and fungi. We find that the model only adequately reproduces the vertical SOM C:P ratio profile when we decrease the microbial P recycling parameter with depth, which results in a decreasing C:P ratio with increasing soil depth. Such a shift in the microbial P recycling parameter indicates the microbial community changes from a nutrient-poor fungi dominance to a nutrient-rich bacteria dominance with depth, which is evidenced by Rousk and Frey (2015), and our model suggests this community shift mainly regulates the SOM C:P ratio decrease in the study site.

N cycle vs. P cycle

The JSM has already reached a quasi-equilibrium state at the end of the 200-year simulations, where the respiration of C and plant uptake of N and P are very close to the C, N, and P from litter fall and SOM accumulates slowly in the soil (Tab.1). The reason for not reaching real equilibrium might firstly be the lack of vegetation feedback, and secondly the constant increasing occluded P pool and decreasing primary P pool do not allow a real equilibrium in JSM, which is also the case for all the TBMs because the same structure of inorganic P cycle from Wang et al. (2010) is used. This will lead to a stability problem especially in long-term simulations, and needs proper investigation in future particularly for the development of soils.

In JSM, the plant nutrient uptake is driven by the root biomass, which is prescribed with the QUINCY outputs, and its uptake capacity, which is taken from the published literature (Kuzyakov and Xu, 2013; Kavka and Polle, 2016). The plant uptake is further influenced by the microbial (and adsorption for P) competition but not regulated by the plant demand due to the absence of vegetation process. The fact that the simulated plant N and P uptake at quasi-equilibrium state are very close to the N and P inputs from the litterfall (Tab.1) indicates that realistic root biomass and uptake capacity enable simulating the nutrient uptake for plant growth. This conclusion supports the recent change of plant uptake simulation in TBMs from plant demand driven (Yang et al., 2014) to trait (root biomass, uptake capacity, and inorganic nutrient pool) driven (Zaehle and Friend, 2010; Goll et al., 2017; Thum et al., 2019), which strengthens interactions between soil nutrient availability and plant growth.

The simulated microbial uptake of inorganic P (238.0 $\mathrm{kgP/ha/yr}$) is not only much higher than the plant P uptake (8.5 $\mathrm{kgP/ha/yr}$), but also much higher than the microbial uptake of inorganic N (Fig.8). This difference is strongly driven by the difference between litter stoichiometry and microbial stoichiometry. In JSM, the nutrient assimilation for microbial growth occurs at two steps, the first one is the microbial DOM uptake in which a certain fraction of N and P (mic_{nue} and mic_{pue}) in the DOM are assimilated directly by microbes, and in the second step microbes further take up the dissolved inorganic N and P through microbial N and P uptake to fulfill their stoichiometry. In the Base Scenario, we used the measured microbial C:N:P ratio of the study site (10.3:0.8:1), which largely differs from the litterfall C:N:P ratio (800:14.8:1), particularly the P content. Therefore, although the demand of N and P for microbial growth do not differ much, the assimilation of dissolved

https://doi.org/10.5194/gmd-2019-187
Preprint. Discussion started: 25 September 2019


Geoscientific Model Development Discussions

organic N is much higher than that of dissolved organic P, resulting in a much higher demand of microbial P uptake than N uptake from the inorganic pool and a very different seasonal pattern of microbial uptake of inorganic N and P (Fig.4). This is well demonstrated in Fig.3 and Fig.8 that the net mineralisation, which equals gross mineralisation minus microbial uptake of inorganic nutrients, is always positive for N and mostly negative for P, especially in the warm season when microbial biomass is high. While the mainity of the gross N mineralisation is taken up by plant, only a minor fraction of the gross P minerlisation is for plant uptake and most of it, together with the extra biomineralsation flux, are taken up by microbes in the form of dissolved inorganic phosphate. This pattern implies that the mobilization of soil N is driven by the plant demand and the mobilization of soil P is driven by the microbial demand.

Microbial stoichiometry

Since we use a very different microbial C:N:P ratio (10.3:0.8:1, Lang et al., 2017) than the global average value (42:6:1, Xu et al., 2013), extra model experiments were conducted with the global microbial stoichiometry to see the effects of microbial C:N:P ratio (Fig.S1-4). The SOC profile and microbial C profile are not significantly different in the new scenarios, but the N&P stocks and fluxes are greatly influenced. One direct consequence of microbial stoichiometry change is the resulted SOM C:N ratio and C:P ratio become lower and higher than the values in the Base Scenario. Moreover, the total demand for microbial N is much higher than the Base Scenario and the demand for microbial P is much lower, leading to a higher microbial uptake of inorganic N and lower microbial uptake of inorganic P, which further imposes changes in the plant-microbe competition of inorganic N and P and the vertical and seasonal patterns of plant and microbial uptake of inorganic nutrients. Although the microbial P demand is lower in the scenario with the global microbial stoichiometry than the Base Scenario, it is still driving the soil P mobilization. However, the N mobilization in the new scenario is no longer only plant-driven but driven by both microbes and plants. This indicates that the microbial stoichiometry is one key factor for soil nutrient processes and plant-soil interactions in JSM.

In JSM, the choice of nutrient mineralisation–immobilization pathways (Manzoni and Porporato, 2009) during microbial DOM uptake, i.e. the microbial nutrient use efficiencies in Eq.S13, does not greatly change the total microbial nutrient assimilation but impose a significant impact on the partitioning between organic (microbial DOM uptake) and inorganic (microbial inorganic nutrient uptake) nutrient assimilation (Tab.2). This partitioning will greatly alter the isotopic signals of the soil pools and is essential to understand the soil nutrient cycling and thus to disentangle the soil effects from the vegetation signals (Craine et al., 2018), something which is not possible in current TBMs due to the poorly defined and parameterised microbial nutrient use efficiencies (Manzoni and Porporato, 2009). It is possible to use JSM to predict realistic microbial nutrient use efficiencies with constrains of tracer experiments data, but needs to be properly investigated in future.

4.2 Key features and model limitations

We apply the ECA approach by Tang and Riley (2013) to simulate the competition for inorganic nutrients. Our model simulations generally indicate that microbes take up moreinorganic P than plants, which agrees with the finding from ^{33}P addition experiments at two other beech forests in Germany (Spohn et al., 2018). However for N, our study shows that plants take up more inorganic N than microbes (Fig.8A and Fig.S1). This seems to disagree with the field studies of ^{15}N addition (e.g.

https://doi.org/10.5194/gmd-2019-187
Preprint. Discussion started: 25 September 2019

Geoscientific Model Development Discussions

Bloor et al., 2009; Dannenmann et al., 2016), and a modelling study using the same approach to simulate competition (Zhu et al., 2017). The reason for this disagreement is that in JSM, we assumed a high microbial N use efficiency of DOM and the main part of microbial N assimilation is actually fulfilled by DOM uptake. Plants therefore take up less inorganic N than microbes. However, in ^{15}N addition experiments and the model study by Zhu et al. (2017), there is no distinction between the assimilation from the organic source and inorganic source, thus the microbes outcompete plants in the sense that the total N assimilated by microbes exceeds total N taken up by the roots, which is also ture in this study. One other uncertainty of the plant-microbe competition for inorganic N is the microbial stoichiometry we used in the parameterisation. As discussed in the previous section, the change of microbial stoichiometry from the field observed value to the global average value can switch the system from microbes outcompeting plant for inorganic N to the opposite. Additionally, the choice of microbial nutrient use efficiencies will not only affect the microbial demand for inorganic nutrients, but also affect the concentrations of inorganic N & P and thus the potential uptake rates of microbes and roots.

We extended the enzyme allocation approach of the SEAM model (Wutzler et al., 2017) by including P and vertical explicitness and assuming a steady state of enzyme production. Due to the very small microbial C:P ratio used in the model parameterisation, our results indicate that the depolymerisation process is solely driven by P demand and thus microbial residues are the preferred substrate because they have a much lower C:P ratio than polymeric litter. It is also supported by the huge P biomineralisation flux (Fig.8), which is independent of depolymerisation and gross mineralisation, and shows that the microbial growth is strongly P limited. Even in the scenario using the global microbial stoichiometry, the depolymerisation is still solely P driven and P biomineralisation supplies more than half of the microbial P demand (Fig.S4). This is partly supported by the global enzymatic activity data that the global ratios of specific C, N and P acquisition activities converged on 1 : 1 : 1 (Sinsabaugh et al., 2008) while the global microbial stoichiometry is much higher, indicating relatively more resources are allocated to acquire P than N and C. This actually reveals a caveat in the current implementation of enzyme allocation in JSM, that the main process to hydrolyze organic P, biomineralisation, is not included in the enzyme allocation calculation. It also explains why the difference between Base Scenario and the enzyme allocation turned-off (SEAM-Off) scenario is very small.

The JSM shows the capacity to (re)produce the vertical and seasonal patterns of the soil stocks and biogeochemical fluxes. While the seasonal patterns are primarily driven by the temperature response of the represented processes, the vertical patterns are shaped by the combined effect of biochemical factors and geophysical factors represented in the model. As seen in Fig.2 and Fig.7, although the total SOC decreases with soil depth, the microbial, litter, and MOC components showed very different patterns. Following the COMISSION model(Ahrens et al., In prep.), in JSM we constrain the capacity of organo-mineral association with the silt and clay content and soil bulk density (BD). In the organic layer and top soil, the continuous litter input sustains a large microbial biomass and microbial residue pool, but due to the very low BD and its relatively low silt and clay content, the sorption is weak and the MOC content is very low. As the soil depth increases, the BD and the silt & clay content both increases so that microbial residues and DOM are more strongly stabilized. This hinders the microbial assimilation of DOM and the immobilization of nutrients, and leads to a strong decline in microbial biomass and an increase in MOC. As a consequence of the decreasing microbial biomass and decreasing litter inputs, there is much less microbial residue and DOM to be sorbed to the mineral soil, which causes the observed decrease of total SOC in deep soil.

https://doi.org/10.5194/gmd-2019-187
Preprint. Discussion started: 25 September 2019

Geoscientific Model Development Discussions

However, there are some caveats need to be mentioned about this study and the JSM model. First, the effects of initial condition and the simulation length on the inorganic P cycle. As indicated by Ahrens et al. (2015), a very long simulation time (13,500 years) is required to reconcile both the measured $\Delta^{14}C$ profile and SOC profile at a nearby Norway spruce forest site. But such a long simulation time is unrealistic for JSM due to the unknown condition of soil inorganic P pools and the un-equilibrated soil inroganic P cycling processes (Yang et al., 2014). Although we use a much shorter simulation length in this study, there are still noticeable uncertainties due to the inorganic P cycling parameters. Second, the model representation of microbial adaptation schemes. In JSM we describe one of the schemes of microbial adaptation proposed by Mooshammer et al. (2014), enzyme allocation, but as mentioned above, the allocation to phosphatase might be essential and needs to be included. Additionally we also find that one other adaptation scheme, the microbial community shift between fungal and bacteria, is very important to reproduce the vertical pattern of soil stoichiometry. Although we mimic such shift in this study by calibration and parameterisation, a more mechanistic representation is necessary in future for representing the acclimation of SOM to climate and environmental changes. Last but not least, given the good quality of the input data, the JSM can adequately reproduce the soil stocks and flux rates at the chosen study site, but the capacity of extrapolation to other climate and soil conditions need to be further investigated in future.

The JSM is overall highly non-linear and sensitive to parameters controlling microbial growth and decay (Tab.2). The C and N stocks in SOM, as well as the respiration and net N mineralisation, are more sensitive to the parameter changes of depolymerisation and organo-mineral association, whereas the stocks of organic/inorganic P and P mineralisation respond more strongly to the microbial processes. This supports, and also explains, the finding of Yang and Post (2011) and Tipping et al. (2016) that the P cycle is decoupled from C and N cycles in the soil. A more in-depth explanation for this difference, as seen from our results, is that the gross mineralisation associated with microbial DOM uptake could supply microbes and plant with sufficient N but not P, thus a huge amount of P needs to be mobilized, especially from SOM but also from mineral pools, to sustain microbial growth. Therefore the microbial pools and soil P stocks/fluxes show high sensitivities to microbial processes.

5 Summary and future directions

We presented the mathematical formulation of a new SOC model, JSM, which extends the vertically explicit, microbial based, and organo-mineral association enabled SOC model, COMISSION, with the N and P processes using novel approaches such as optimized enzyme allocation, nutrient acquisition competition, and processes acclimation. The model was evaluated with the observed C, N, and P stocks of SOM, soil inorganic P stock, microbial C, N, and P contents, and soil bulk density of the topmost 1m soil from a German beech forest and demonstrated that it is capable of capturing the sizes and vertical patterns of the observations. We further presented the main features of nutrient cycling under the new model structure and the sensitivities of model outputs to parameter changes. Both of them indicate that the P cycle is decoupled from the C-N cycle and has very strong interactions with microbial dynamics. The evaluation of model experiments points to the need of better representing interactions between P cycle and microbial dynamics in JSM.

https://doi.org/10.5194/gmd-2019-187
Preprint. Discussion started: 25 September 2019

The next step of the model evaluation is to investigate the effects of P cycling on microbial dynamics and SOM cycling more in depth by subjecting it to other beech forest sites in Germany along a soil P availability gradient, and to evaluate if the contrasting P cycling patterns proposed by Lang et al. (2017) as "acquiring system" and "recycling system" can be reproduced by the model. Such model evaluation is expected to identify the key/missing processes of the model to reproduce the contrasting P cycling schemes, and how these processes influence the turnover/stability of SOM.

JSM is developed under the framework of the new biosphere model, QUINCY, and the future plan is to apply this model coupled with the vegetation component of the QUINCY model by Thum et al. (2019), which will allow us to have an alternative to better represent the interactions between root growth/activity and SOM turnover and stabilisation in terrestrial biosphere models.

Code availability. The JSM model is developed using the QUINCY modelling framework and is licensed under GNU GPL version 3. The scientific code of JSM requires software from the MPI-ESM environment, which is subject to the MPI-M-Software-License-Agreement in its most recent form (http://www.mpimet.mpg.de/en/science/models/license). The source code is available online (https://git.bgc-jena.mpg.de/quincy/quincy-model-release, branch "jsm/release01"), but its access is restricted to registered users. Readers interested in running the model should request a username and password from the corresponding authors or via the git-repository. Model users are strongly encouraged to follow the fair-use policy stated on https://www.bgc-jena.mpg.de/bgi/index.php/Projects/QUINCYModel.

Author contributions. SZ conceived the model. LY and SZ developed the model. MS collected the observation data. All authors contributed to the interpretation of the results and writing of the manuscript.

Acknowledgements. This work was supported by the framework of Priority Program SPP 1685 “Ecosystem Nutrition: Forest Strategies for Limited Phosphorus Resources” of the German Research Foundation (DFG), grant No.ZA 763/2-1. We are grateful to Jan Engel for technical assistance in developing the code, and to Marleen Pallandt for improving the quality of the manuscript.

https://doi.org/10.5194/gmd-2019-187
Preprint. Discussion started: 25 September 2019

Geoscientific Model Development Discussions

References

Ahrens, B., Braakhekke, M. C., Guggenberger, G., Schrumpf, M., and Reichstein, M.: Contribution of sorption, DOC transport and microbial interactions to the 14C age of a soil organic carbon profile: Insights from a calibrated process model, Soil Biology and Biochemistry, 88, 390–402, https://doi.org/10.1016/j.soilbio.2015.06.008, http://dx.doi.org/10.1016/j.soilbio.2015.06.008, 2015.

Ahrens, B., Reichstein, M., Guggenberger, G., and Schrumpf, M.: Towards reconciling radiocarbon and carbon in soils: the importance of modelling organo-mineral associations, In prep.

Allison, S. D. and Vitousek, P. M.: Responses of extracellular enzymes to simple and complex nutrient inputs, Soil Biology and Biochemistry, 37, 937–944, https://doi.org/https://doi.org/10.1016/j.soilbio.2004.09.014, http://www.sciencedirect.com/science/article/pii/S0038071704004080, 2005.

Barrow, N. J.: The description of phosphate adsorption curves, Journal of Soil Science, 29, 447–462, 1978.

Bergkemper, F., Bunemann, E. K., Hauenstein, S., Heuck, C., Kandeler, E., Kruger, J., Marhan, S., Meszaros, E., Nassal, D., Nassal, P., Oelmann, Y., Pistocchi, C., Schloter, M., Spohn, M., Talkner, U., Zederer, D. P., and Schulz, S.: An inter-laboratory comparison of gaseous and liquid fumigation based methods for measuring microbial phosphorus (Pmic) in forest soils with differing P stocks, Journal of Microbiological Methods, 128, 66–68, https://doi.org/10.1016/j.mimet.2016.07.006, https://www.ncbi.nlm.nih.gov/pubmed/27422116, 2016.

Blagodatskaya, E. and Kuzyakov, Y.: Mechanisms of real and apparent priming effects and their dependence on soil microbial biomass and community structure: critical review, Biology and Fertility of Soils, 45, 115–131, https://doi.org/10.1007/s00374-008-0334-y, 2008.

Bloor, J. M. G., Niboyet, A., Leadley, P. W., and Barthes, L.: CO2 and inorganic N supply modify competition for N between co-occurring grass plants, tree seedlings and soil microorganisms, Soil Biology and Biochemistry, 41, 544–552, https://doi.org/https://doi.org/10.1016/j.soilbio.2008.12.013, http://www.sciencedirect.com/science/article/pii/S0038071708004537, 2009.

Bond-Lamberty, B., Bailey, V. L., Chen, M., Gough, C. M., and Vargas, R.: Globally rising soil heterotrophic respiration over recent decades, Nature, 560, 80–83, https://doi.org/10.1038/s41586-018-0358-x, https://doi.org/10.1038/s41586-018-0358-x, 2018.

Bradford, M. A., Wieder, W. R., Bonan, G. B., Fierer, N., Raymond, P. A., and Crowther, T. W.: Managing uncertainty in soil carbon feedbacks to climate change, Nature Climate Change, 6, 751, https://doi.org/10.1038/nclimate3071, https://doi.org/10.1038/nclimate3071, 2016.

Bünemann, E. K., Augstburger, S., and Frossard, E.: Dominance of either physicochemical or biological phosphorus cycling processes in temperate forest soils of contrasting phosphate availability, Soil Biology and Biochemistry, 101, 85–95, https://doi.org/10.1016/j.soilbio.2016.07.005, 2016.

Ciais, P., Sabine, C., Bala, G., Bopp, L., Brovkin, V., Canadell, J., Chhabra, A., DeFries, R., Galloway, J., Heimann, M., Jones, C., Quéré, C. L., Myneni, R. B., Piao, S., and Thornton, P.: Carbon and Other Biogeochemical Cycles, pp. 465–570, Cambridge University Press, Cambridge, United Kingdom and New York, NY, USA, https://doi.org/10.1017/CBO9781107415324.015, http://www.ipcc.ch/report/ar5/wg1/docs/review/WG1AR5_SOD_Ch06_All_Final.pdf%5Cnhttp://ebooks.cambridge.org/ref/id/CBO9781107415324A023, 2013.

Craine, J. M., Morrow, C., and Fierer, N.: Microbial nitrogen limitation increases decomposition, Ecology, 88, 2105–2113, https://doi.org/10.1890/06-1847.1, https://doi.org/10.1890/06-1847.1, 2007.

Craine, J. M., Elmore, A. J., Wang, L., Aranibar, J., Bauters, M., Boeckx, P., Crowley, B. E., Dawes, M. A., Delzon, S., Fajardo, A., Fang, Y., Fujiyoshi, L., Gray, A., Guerrieri, R., Gundale, M. J., Hawke, D. J., Hietz, P., Jonard, M., Kearsley, E., Kenzo, T., Makarov, M., Marañón-Jiménez, S., McGlynn, T. P., McNeil, B. E., Mosher, S. G., Nelson, D. M., Peri, P. L., Roggy, J. C., Sanders-DeMott, R., Song,

https://doi.org/10.5194/gmd-2019-187
Preprint. Discussion started: 25 September 2019

M., Szpak, P., Templer, P. H., Van der Colff, D., Werner, C., Xu, X., Yang, Y., Yu, G., and Zmudczyńska-Skarbek, K.: Isotopic evidence for oligotrophication of terrestrial ecosystems, Nature Ecology & Evolution, 2, 1735–1744, https://doi.org/10.1038/s41559-018-0694-0, https://doi.org/10.1038/s41559-018-0694-0, 2018.

Dannenmann, M., Bimüller, C., Gschwendtner, S., Leberecht, M., Tejedor, J., Bilela, S., Gasche, R., Hanewinkel, M., Baltensweiler, A., Kögel-Knabner, I., Polle, A., Schloter, M., Simon, J., and Rennenberg, H.: Climate Change Impairs Nitrogen Cycling in European Beech Forests, PLOS ONE, 11, e0158 823, https://doi.org/10.1371/journal.pone.0158823, https://doi.org/10.1371/journal.pone.0158823, 2016.

Davidson, E. A., Samanta, S., Caramori, S. S., and Savage, K.: The Dual Arrhenius and Michaelis-Menten kinetics model for decomposition of soil organic matter at hourly to seasonal time scales, Glob. Change Biol., 18, 371–384, 2012.

Drake, J. E., Gallet-Budynek, A., Hofmockel, K. S., Bernhardt, E. S., Billings, S. A., Jackson, R. B., Johnsen, K. S., Lichter, J., McCarthy, H. R., McCormack, M. L., Moore, D. J. P., Oren, R., Palmroth, S., Phillips, R. P., Pippen, J. S., Pritchard, S. G., Treseder, K. K., Schlesinger, W. H., DeLucia, E. H., and Finzi, A. C.: Increases in the flux of carbon belowground stimulate nitrogen uptake and sustain the long-term enhancement of forest productivity under elevated CO2, Ecology Letters, 14, 349–357, https://doi.org/10.1111/j.1461-0248.2011.01593.x, https://doi.org/10.1111/j.1461-0248.2011.01593.x, 2011.

Ellsworth, D., Anderson, I., Crous, K., Cooke, J., Drake, J., Gherlenda, A., Gimeno, T., Macdonald, C., Medlyn, B., Powell, J., Tjoelker, M., and Reich, P.: Elevated CO2 does not increase eucalypt forest productivity on a low-phosphorus soil, Nature Climate Change, 7, 279–282, https://doi.org/10.1038/nclimate3235, 2017.

Federer, C. A., Turcotte, D. E., and Smith, C. T.: The organic fraction–bulk density relationship and the expression of nutrient content in forest soils, Canadian Journal of Forest Research, 23, 1026–1032, https://doi.org/10.1139/x93-131, https://doi.org/10.1139/x93-131, 1993.

Fujita, K., Kunito, T., Moro, H., Toda, H., Otsuka, S., and Nagaoka, K.: Microbial resource allocation for phosphatase synthesis reflects the availability of inorganic phosphorus across various soils, Biogeochemistry, 136, 325–339, https://doi.org/10.1007/s10533-017-0398-6, https://doi.org/10.1007/s10533-017-0398-6, 2017.

Goll, D. S., Vuichard, N., Maignan, F., Jornet-Puig, A., Sardans, J., Violette, A., Peng, S., Sun, Y., Kvakic, M., Guimberteau, M., Guenet, B., Zaehle, S., Penuelas, J., Janssens, I., and Ciais, P.: A representation of the phosphorus cycle for ORCHIDEE (revision 4520), Geosci. Model Dev., 10, 3745–3770, https://doi.org/10.5194/gmd-10-3745-2017, https://www.geosci-model-dev.net/10/3745/2017/, 2017.

Hinsinger, P., Brauman, A., Devau, N., Gérard, F., Jourdan, C., Laclau, J.-P., Le Cadre, E., Jaillard, B., and Plassard, C.: Acquisition of phosphorus and other poorly mobile nutrients by roots. Where do plant nutrition models fail?, Plant and Soil, 348, 29–61, https://doi.org/10.1007/s11104-011-0903-y, 2011.

Hou, E., Chen, C., Luo, Y., Zhou, G., Kuang, Y., Zhang, Y., Heenan, M., Lu, X., and Wen, D.: Effects of climate on soil phosphorus cycle and availability in natural terrestrial ecosystems, Global Change Biology, 24, 3344–3356, https://doi.org/10.1111/gcb.14093, https://doi.org/10.1111/gcb.14093, 2018.

Iversen, C. M., Keller, J. K., Garten Jr, C. T., and Norby, R. J.: Soil carbon and nitrogen cycling and storage throughout the soil profile in a sweetgum plantation after 11 years of CO2-enrichment, Global Change Biology, 18, 1684–1697, https://doi.org/10.1111/j.1365-2486.2012.02643.x, https://doi.org/10.1111/j.1365-2486.2012.02643.x, 2012.

Jackson, R. B., Canadell, J., Ehleringer, J. R., Mooney, H. A., Sala, O. E., and Schulze, E. D.: A global analysis of root distributions for terrestrial biomes, Oecologia, 108, 389–411, https://doi.org/10.1007/BF00333714, https://doi.org/10.1007/BF00333714, 1996.

Jonard, M., Fürst, A., Verstraeten, A., Thimonier, A., Timmermann, V., Potočić, N., Waldner, P., Benham, S., Hansen, K., Merilä, P., Ponette, Q., de la Cruz, A. C., Roskams, P., Nicolas, M., Croisé, L., Ingerslev, M., Matteucci, G., Decinti, B., Bascietto, M., and Rautio, P.: Tree mineral nutrition is deteriorating in Europe, Global Change Biology, 21, 418–430, https://doi.org/10.1111/gcb.12657, 2015.

https://doi.org/10.5194/gmd-2019-187
Preprint. Discussion started: 25 September 2019

Kavka, M. and Polle, A.: Phosphate uptake kinetics and tissue-specific transporter expression profiles in poplar (Populus × canescens) at different phosphorus availabilities, BMC Plant Biology, 16, 206, https://doi.org/10.1186/s12870-016-0892-3, https://doi.org/10.1186/s12870-016-0892-3, 2016.

Koven, C. D., Riley, W. J., Subin, Z. M., Tang, J. Y., Torn, M. S., Collins, W. D., Bonan, G. B., Lawrence, D. M., and Swenson, S. C.: The effect of vertically resolved soil biogeochemistry and alternate soil C and N models on C dynamics of CLM4, Biogeosciences, 10, 7109–7131, 2013.

Kuzyakov, Y. and Xu, X.: Competition between roots and microorganisms for nitrogen: mechanisms and ecological relevance, New Phytologist, 198, 656–669, https://doi.org/doi:10.1111/nph.12235, https://nph.onlinelibrary.wiley.com/doi/abs/10.1111/nph.12235, 2013.

Lang, F., Krüger, J., Amelung, W., Willbold, S., Frossard, E., Bünemann, E. K., Bauhus, J., Nitschke, R., Kandeler, E., Marhan, S., Schulz, S., Bergkemper, F., Schloter, M., Luster, J., Guggisberg, F., Kaiser, K., Mikutta, R., Guggenberger, G., Polle, A., Pena, R., Prietzel, J., Rodionov, A., Talkner, U., Meesenburg, H., von Wilpert, K., Hölscher, A., Dietrich, H. P., and Chmara, I.: Soil phosphorus supply controls P nutrition strategies of beech forest ecosystems in Central Europe, Biogeochemistry, https://doi.org/10.1007/s10533-017-0375-0, 2017.

Manzoni, S. and Porporato, A.: Soil carbon and nitrogen mineralization: Theory and models across scales, Soil Biology and Biochemistry, 41, 1355–1379, https://doi.org/10.1016/j.soilbio.2009.02.031, http://linkinghub.elsevier.com/retrieve/pii/S0038071709000765, 2009.

Manzoni, S., Porporato, A., and Schimel, J. P.: Soil heterogeneity in lumped mineralization–immobilization models, Soil Biology and Biochemistry, 40, 1137–1148, 2008.

Manzoni, S., Taylor, P., Richter, A., Porporato, A., and Agren, G. I.: Environmental and stoichiometric controls on microbial carbon-use efficiency in soils, New Phytol, 196, 79–91, https://doi.org/10.1111/j.1469-8137.2012.04225.x, https://www.ncbi.nlm.nih.gov/pubmed/22924405, 2012.

McCarthy, H. R., Oren, R., Johnsen, K. H., Gallet-Budynek, A., Pritchard, S. G., Cook, C. W., LaDeau, S. L., Jackson, R. B., and Finzi, A. C.: Re-assessment of plant carbon dynamics at the Duke free-air CO2 enrichment site: interactions of atmospheric [CO2] with nitrogen and water availability over stand development, New Phytologist, 185, 514–528, https://doi.org/10.1111/j.1469-8137.2009.03078.x, https://doi.org/10.1111/j.1469-8137.2009.03078.x, 2010.

Medlyn, B. E., Zaehle, S., De Kauwe, M. G., Walker, A. P., Dietze, M. C., Hanson, P. J., Hickler, T., Jain, A. K., Luo, Y., Parton, W., Prentice, I. C., Thornton, P. E., Wang, S., Wang, Y.-P., Weng, E., Iversen, C. M., McCarthy, H. R., Warren, J. M., Oren, R., and Norby, R. J.: Using ecosystem experiments to improve vegetation models, Nature Climate Change, 5, 528, https://doi.org/10.1038/nclimate2621, https://doi.org/10.1038/nclimate2621, 2015.

Medlyn, B. E., De Kauwe, M. G., Zaehle, S., Walker, A. P., Duursma, R. A., Luus, K., Mishurov, M., Pak, B., Smith, B., Wang, Y.-P., Yang, X., Crous, K. Y., Drake, J. E., Gimeno, T. E., Macdonald, C. A., Norby, R. J., Power, S. A., Tjoelker, M. G., and Ellsworth, D. S.: Using models to guide field experiments: a priori predictions for the CO2 response of a nutrient- and water-limited native Eucalypt woodland, Global Change Biology, 22, 2834–2851, https://doi.org/10.1111/gcb.13268, https://doi.org/10.1111/gcb.13268, 2016.

Mooshammer, M., Wanek, W., Zechmeister-Boltenstern, S., and Richter, A.: Stoichiometric imbalances between terrestrial decomposer communities and their resources: mechanisms and implications of microbial adaptations to their resources, Frontiers in Microbiology, 5, https://doi.org/10.3389/fmicb.2014.00022, https://www.frontiersin.org/article/10.3389/fmicb.2014.00022, 2014.

Olander, L. P. and Vitousek, P. M.: Regulation of soil phosphatase and chitinase activity by N and P availability, Biogeochemistry, 49, 175–190, https://doi.org/10.1023/A:1006316117817, 2000.

Parton, W. J., Stewart, J. W. B., and Cole, C. V.: Dynamics of C, N, P and S in grassland soils: a model, Biogeochemistry, 5, 109–131, https://doi.org/10.1007/BF02180320, http://link.springer.com/10.1007/BF02180320, 1988.

https://doi.org/10.5194/gmd-2019-187
Preprint. Discussion started: 25 September 2019

Parton, W. J., Scurlock, J. M. O., Ojima, D. S., Gilmanov, T. G., Scholes, R. J., Schimmel, D. S., Kirchner, T., Menaut, J. C., Seastedt, T., Moya, E. G., Kamnalrut, A., and Kinyamario, J. I.: Observations and modelling of biomass and soil organic matter dynamics for the grassland biome worldwide, Global Biogeochemical Cycles, 7, 785–809, 1993.

Rousk, J. and Frey, S. D.: Revisiting the hypothesis that fungal-to-bacterial dominance characterizes turnover of soil organic matter and nutrients, Ecological Monographs, 85, 457–472, https://doi.org/10.1890/14-1796.1, https://doi.org/10.1890/14-1796.1, 2015.

Saltelli, A., Chan, K., and Scott, E. M.: Sensitivity Analysis, John Wiley & Sons, ltd., Chichester, New York, 2000.

Schimel, J. P. and Weintraub, M. N.: The implications of exoenzyme activity on microbial carbon and nitrogen limitation in soil: A theoretical model, Soil Biology and Biochemistry, 35, 549–563, https://doi.org/10.1016/S0038-0717(03)00015-4, http://linkinghub.elsevier.com/retrieve/pii/S0038071703000154, 2003.

Schmidt, M. W. I., Torn, M. S., Abiven, S., Dittmar, T., Guggenberger, G., Janssens, I. a., Kleber, M., Kögel-Knabner, I., Lehmann, J., Manning, D. a. C., Nannipieri, P., Rasse, D. P., Weiner, S., and Trumbore, S. E.: Persistence of soil organic matter as an ecosystem property, Nature, 478, 49–56, https://doi.org/10.1038/nature10386, 2011.

Sinsabaugh, R. L., Lauber, C. L., Weintraub, M. N., Ahmed, B., Allison, S. D., Crenshaw, C., Contosta, A. R., Cusack, D., Frey, S., Gallo, M. E., Gartner, T. B., Hobbie, S. E., Holland, K., Keeler, B. L., Powers, J. S., Stursova, M., Takacs-Vesbach, C., Waldrop, M. P., Wallenstein, M. D., Zak, D. R., and Zeglin, L. H.: Stoichiometry of soil enzyme activity at global scale, Ecology Letters, 11, 1252–1264, https://doi.org/10.1111/j.1461-0248.2008.01245.x, http://www.ncbi.nlm.nih.gov/pubmed/18823393, 2008.

Sinsabaugh, R. L., Turner, B. L., Talbot, J. M., Waring, B. G., Powers, J. S., Kuske, C. R., Moorhead, D. L., and Follstad Shah, J. J.: Stoichiometry of microbial carbon use efficiency in soils, Ecological Monographs, 86, 172–189, https://doi.org/10.1890/15-2110.1, http://dx.doi.org/10.1890/15-2110.1, 2016.

Smith, B., Wärlind, D., Arneth, A., Hickler, T., Leadley, P., Siltberg, J., and Zaehle, S.: Implications of incorporating N cycling and N limitations on primary production in an individual-based dynamic vegetation model, Biogeosciences, 11, 2027–2054, https://doi.org/10.5194/bg-11-2027-2014, http://www.biogeosciences.net/11/2027/2014/, 2014.

Spohn, M., Zavišić, A., Nassal, P., Bergkemper, F., Schulz, S., Marhan, S., Schloter, M., Kandeler, E., and Polle, A.: Temporal variations of phosphorus uptake by soil microbial biomass and young beech trees in two forest soils with contrasting phosphorus stocks, Soil Biology and Biochemistry, 117, 191–202, https://doi.org/https://doi.org/10.1016/j.soilbio.2017.10.019, http://www.sciencedirect.com/science/article/pii/S003807171730620X, 2018.

Sulman, B. N., Moore, J. A. M., Abramoff, R., Averill, C., Kivlin, S., Georgiou, K., Sridhar, B., Hartman, M. D., Wang, G., Wieder, W. R., Bradford, M. A., Luo, Y., Mayes, M. A., Morrison, E., Riley, W. J., Salazar, A., Schimel, J. P., Tang, J., and Classen, A. T.: Multiple models and experiments underscore large uncertainty in soil carbon dynamics, Biogeochemistry, 141, 109–123, https://doi.org/10.1007/s10533-018-0509-z, https://doi.org/10.1007/s10533-018-0509-z, 2018.

Tang, J. Y. and Riley, W. J.: A total quasi-steady-state formulation of substrate uptake kinetics in complex networks and an example application to microbial litter decomposition, Biogeosciences, 10, 8329–8351, https://doi.org/10.5194/bg-10-8329-2013, <GotoISI>://WOS:000329054600033, 2013.

Thornton, P. E., Lamarque, J.-F., Rosenbloom, N. A., and Mahowald, N. M.: Influence of carbon-nitrogen cycle coupling on land model response to CO2 fertilization and climate variability, Global Biogeochemical Cycles, 21, https://doi.org/10.1029/2006GB002868, https://doi.org/10.1029/2006GB002868, 2007.

https://doi.org/10.5194/gmd-2019-187
Preprint. Discussion started: 25 September 2019

Thum, T., Caldararu, S., Engel, J., Kern, M., Pallandt, M., Yu, L., and Zaehle, S.: A new terrestrial ecosystem model with coupled carbon, nitrogen, and phosphorus cycles (QUINCY v1.0; revision 1610), https://projects.bgc-jena.mpg.de/QUINCY/browser/project-A/tags/tag1, 2019.

Tipping, E., Somerville, C. J., and Luster, J.: The C:N:P:S stoichiometry of soil organic matter, Biogeochemistry, 130, 117–131, https://doi.org/10.1007/s10533-016-0247-z, 2016.

Van der Zee, S., Leus, F., and Louer, M.: Prediction of phosphate transport in small columns with an approximate sorption kinetics model, Water Resources Research, 25, 1353–1365, 1989.

Wang, G., Post, W. M., Mayes, M. A., Frerichs, J. T., and Sindhu, J.: Parameter estimation for models of ligninolytic and cellulolytic enzyme kinetics, Soil Biology and Biochemistry, 48, 28–38, https://doi.org/https://doi.org/10.1016/j.soilbio.2012.01.011, http://www.sciencedirect.com/science/article/pii/S0038071712000247, 2012.

Wang, G., Post, W. M., and Mayes, M. A.: Development of microbial-enzyme-mediated decomposition model parameters through steady-state and dynamic analyses, Ecological Applications, 23, 255–272, https://doi.org/10.1890/12-0681.1, https://esajournals.onlinelibrary.wiley.com/doi/abs/10.1890/12-0681.1, 2013.

Wang, Y. P., Law, R. M., and Pak, B.: A global model of carbon, nitrogen and phosphorus cycles for the terrestrial biosphere, Biogeosciences, 7, 2261–2282, 2010.

Warren, J. M., Pötzelsberger, E., Wullschleger, S. D., Thornton, P. E., Hasenauer, H., and Norby, R. J.: Ecohydrologic impact of reduced stomatal conductance in forests exposed to elevated CO2, Ecohydrology, 4, 196–210, https://doi.org/10.1002/eco.173, https://doi.org/10.1002/eco.173, 2011.

White, M. A., Thornton, P. E., Running, S., and Nemani, R.: Parameterization and Sensitivity Analysis of the BIOME-BGC Terrestrial Ecosystem Model: Net Primary Production Controls, Earth Interactions, 4, 1–55, 2000.

WRB, I. W. G.: World Reference Base for Soil Resources 2014, update 2015. International soil classification system for naming soils and creating legends for soil maps., Report, 2015.

Wutzler, T., Zaehle, S., Schrumpf, M., Ahrens, B., and Reichstein, M.: Adaptation of microbial resource allocation affects modelled long term soil organic matter and nutrient cycling, Soil Biology and Biochemistry, 115, 322–336, https://doi.org/https://doi.org/10.1016/j.soilbio.2017.08.031, http://www.sciencedirect.com/science/article/pii/S0038071717305680, 2017.

Xu, X., Thornton, P. E., and Post, W. M.: A global analysis of soil microbial biomass carbon, nitrogen and phosphorus in terrestrial ecosystems, Global Ecology and Biogeography, 22, 737–749, https://doi.org/10.1111/geb.12029, https://doi.org/10.1111/geb.12029, 2013.

Yang, X. and Post, W. M.: Phosphorus transformations as a function of pedogenesis: A synthesis of soil phosphorus data using Hedley fractionation method, Biogeosciences, 8, 2907–2916, https://doi.org/10.5194/bg-8-2907-2011, 2011.

Yang, X., Post, W. M., Thornton, P. E., and Jain, A.: The distribution of soil phosphorus for global biogeochemical modeling, Biogeosciences, 10, 2525–2537, https://doi.org/10.5194/bg-10-2525-2013, 2013.

Yang, X., Thornton, P. E., Ricciuto, D. M., and Post, W. M.: The role of phosphorus dynamics in tropical forests – a modeling study using CLM-CNP, Biogeosciences, 11, 1667–1681, https://doi.org/10.5194/bg-11-1667-2014, https://www.biogeosciences.net/11/1667/2014/, 2014.

Yu, L., Zanchi, G., Akselsson, C., Wallander, H., and Belyazid, S.: Modeling the forest phosphorus nutrition in a southwestern Swedish forest site, Ecological Modelling, 369, 88–100, https://doi.org/https://doi.org/10.1016/j.ecolmodel.2017.12.018, http://www.sciencedirect.com/science/article/pii/S030438001730501X, 2018.

https://doi.org/10.5194/gmd-2019-187
Preprint. Discussion started: 25 September 2019

Zaehle, S. and Friend, A. D.: Carbon and nitrogen cycle dynamics in the O-CN land surface model: 1. Model description, site-scale evaluation, and sensitivity to parameter estimates, Global Biogeochemical Cycles, 24, https://doi.org/10.1029/2009GB003521, https://doi.org/10.1029/2009GB003521, 2010.

Zaehle, S., Sitch, S. A., Smith, B., and Hatterman, F.: Effects of parameter uncertainties on the modeling of terrestrial biosphere dynamics, Global Biogeochemical Cycles, 19, doi:10.1029–2004GB002 395, https://doi.org/doi:10.1029/2004GB002395, 2005.

Zaehle, S., Medlyn, B. E., De Kauwe, M. G., Walker, A. P., Dietze, M. C., Hickler, T., Luo, Y., Wang, Y.-P., El-Masri, B., Thornton, P., Jain, A., Wang, S., Warlind, D., Weng, E., Parton, W., Iversen, C. M., Gallet-Budynek, A., McCarthy, H., Finzi, A., Hanson, P. J., Prentice, I. C., Oren, R., and Norby, R. J.: Evaluation of 11 terrestrial carbon–nitrogen cycle models against observations from two temperate Free-Air CO2 Enrichment studies, New Phytologist, 202, 803–822, https://doi.org/10.1111/nph.12697, https://doi.org/10.1111/nph.12697, 2014.

Zederer, D. P., Talkner, U., Spohn, M., and Joergensen, R. G.: Microbial biomass phosphorus and C/N/P stoichiometry in forest floor and A horizons as affected by tree species, Soil Biology and Biochemistry, 111, 166–175, https://doi.org/10.1016/j.soilbio.2017.04.009, 2017.

Zhu, Q., Riley, W. J., Tang, J., and Koven, C. D.: Multiple soil nutrient competition between plants, microbes, and mineral surfaces: model development, parameterization, and example applications in several tropical forests, Biogeosciences, 13, 341–363, https://doi.org/10.5194/bg-13-341-2016, 2016.

Zhu, Q., Riley, W. J., and Tang, J.: A new theory of plant–microbe nutrient competition resolves inconsistencies between observations and model predictions, Ecological Applications, 27, 875–886, https://doi.org/10.1002/eap.1490, 2017.

https://doi.org/10.5194/gmd-2019-187
Preprint. Discussion started: 25 September 2019

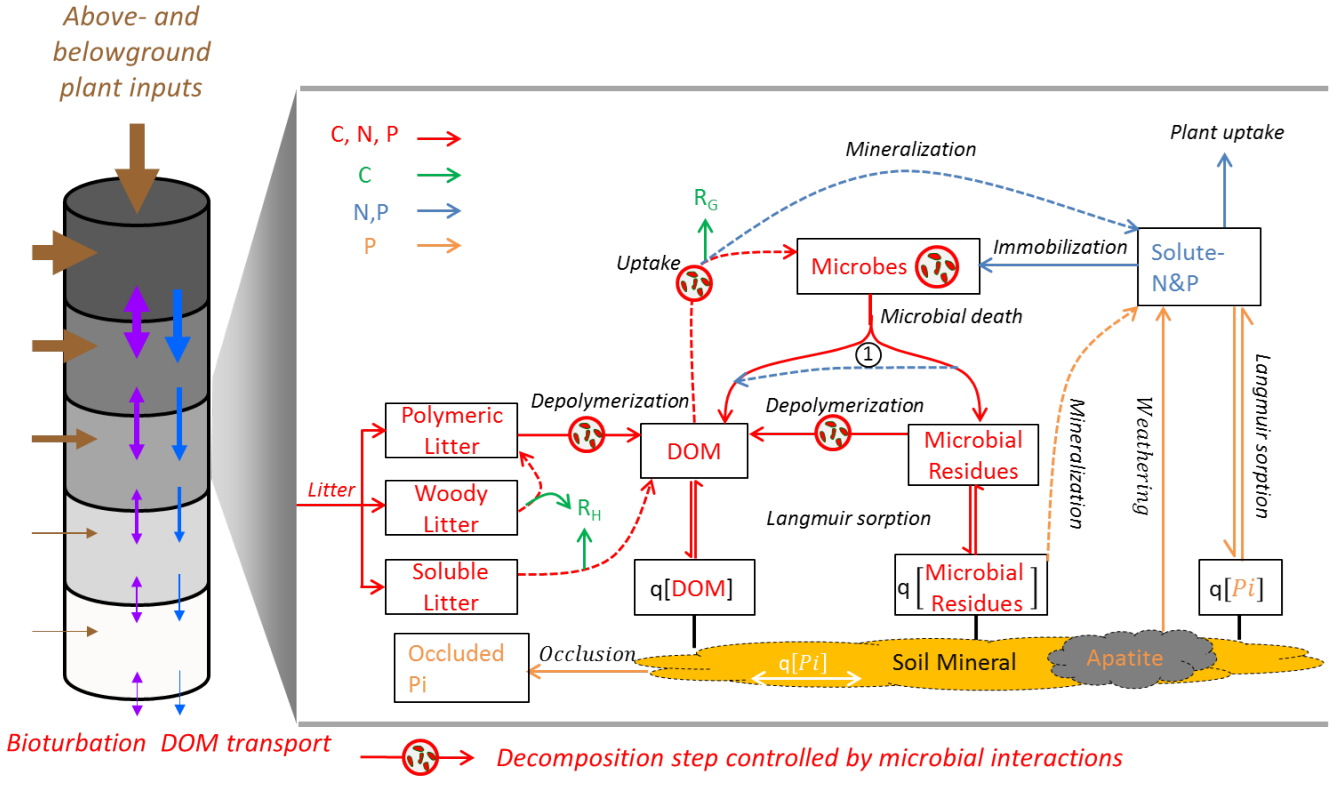

Figure 1. Theoretical representation of Jena Soil Model (JSM) structure. The vertical soil profile (10m) is split into 15 soil layers, aboveground litter is added on top of the soil profile, root litter enters into each soil layer according to the root distribution. Bioturbation and DOM transport translocate SOM between soil layers. In each soil layer, boxes refer to pools and lines refer to processes, in which red lines: biogeochemical fluxes with C, N and P; green lines: respiration fluxes, R_H for heterotrophic respiration and R_G for microbial growth respiration; blue lines: fluxes with N and P; orange lines: fluxes with only P; dashed lines: biogeochemical processes that involves stoichiometry change between sourcing and sinking pools. ①: microbial nutrient recycle from residue to DOM during decay; $q[X]$: mineral-associated form (adsorbed to soil mineral surface, or absorbed into soil mineral matrix) of X, which can be DOM, microbial residues, or inorganic phosphate (Pi).

https://doi.org/10.5194/gmd-2019-187
Preprint. Discussion started: 25 September 2019

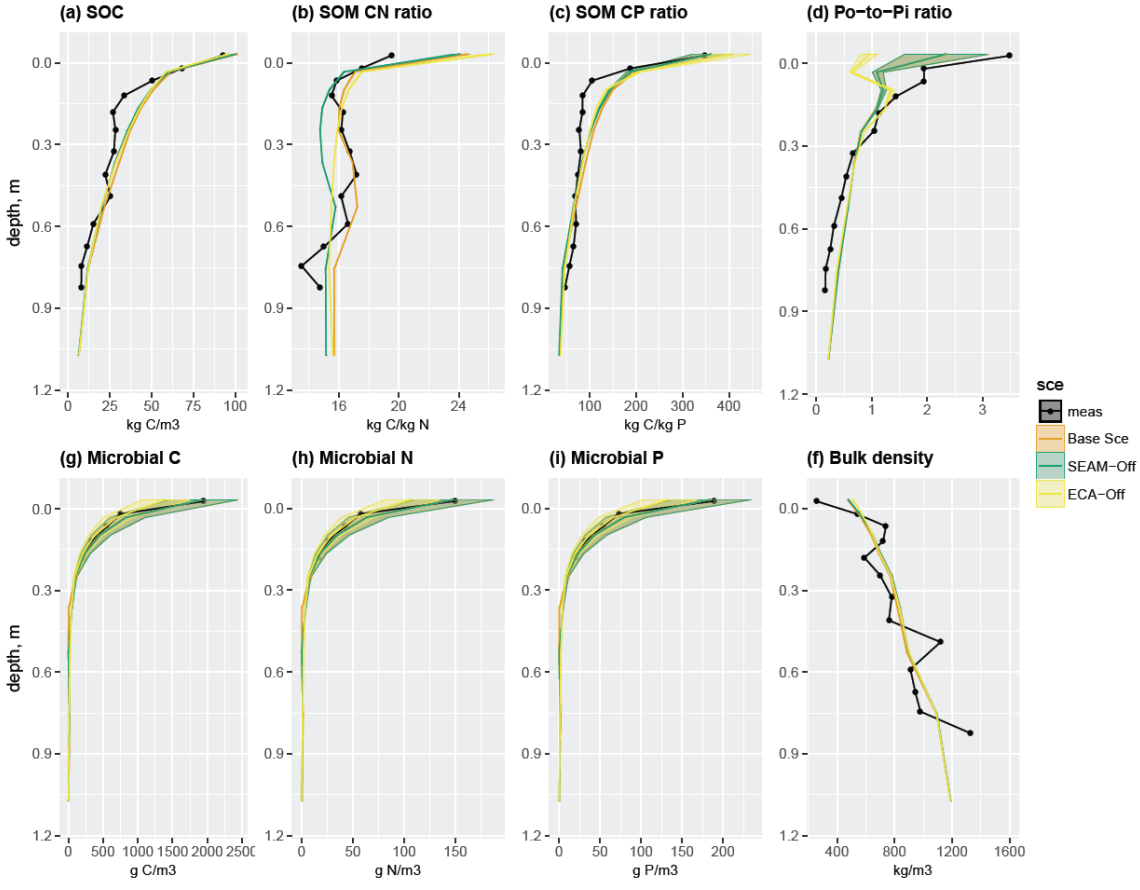

Figure 2. Simulated and observed (a) SOC content, (b) C:N ration in SOM, (c) C:P ratio in SOM, (d) organic P to inorganic P ratio in soil, microbial C, N, and P content ((e) to (g)), and (h) soil bulk density at the study site up to 1m soil depth. Black lines and dots: observations; Color lines and shades: simulated mean values and ranges of standard deviation by different model experiments in Sect.2.3. The microbial C, N, and P are only measured in top 30cm soil. Simulated means and standard deviations are calculated using data of the last 10 years from the model experiments.

https://doi.org/10.5194/gmd-2019-187
Preprint. Discussion started: 25 September 2019

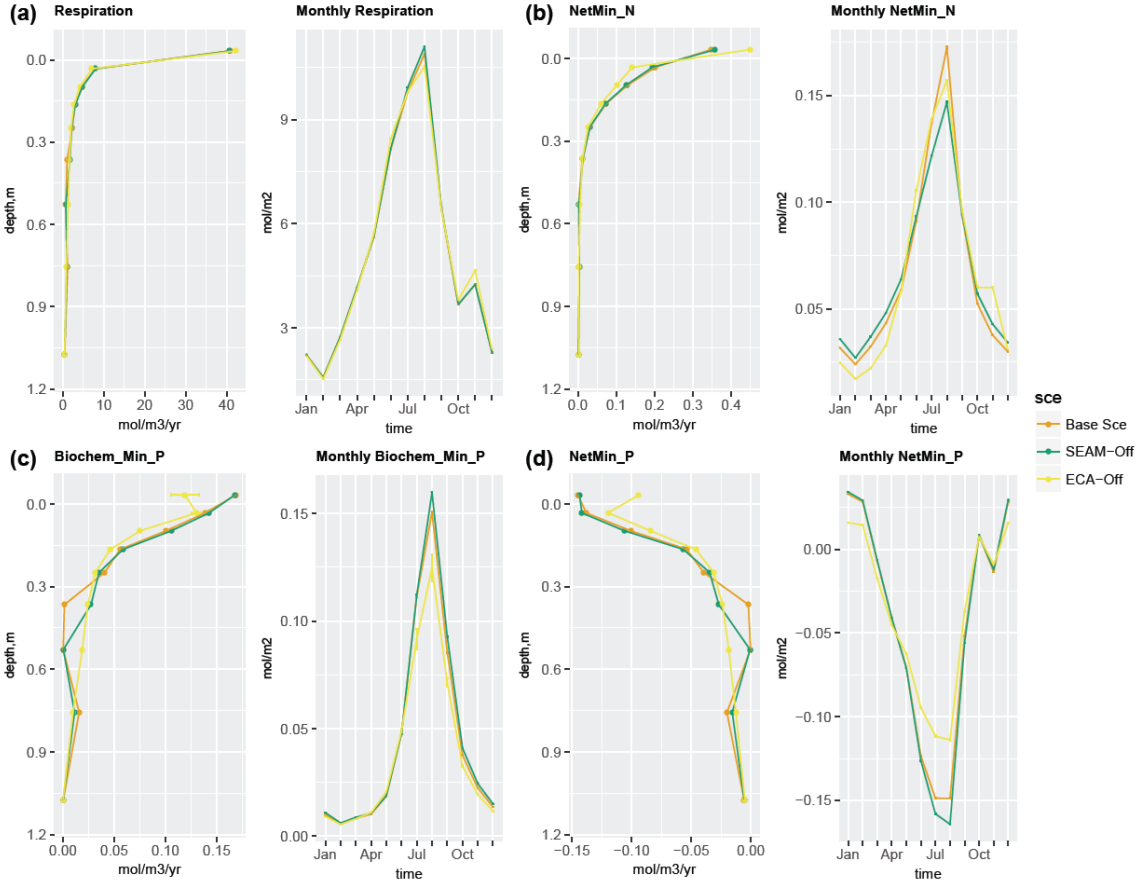

Figure 3. Simulated seasonal and vertical distribution of (a) respiration, (b) net N mineralisation, (c) biochemical P mineralisation, and (d) net P mineralisation at the study site for the whole soil profile. Points represent the mean values and error bars represent the standard deviations, both calculated using data of the last 10 years from the model experiments.

https://doi.org/10.5194/gmd-2019-187
Preprint. Discussion started: 25 September 2019

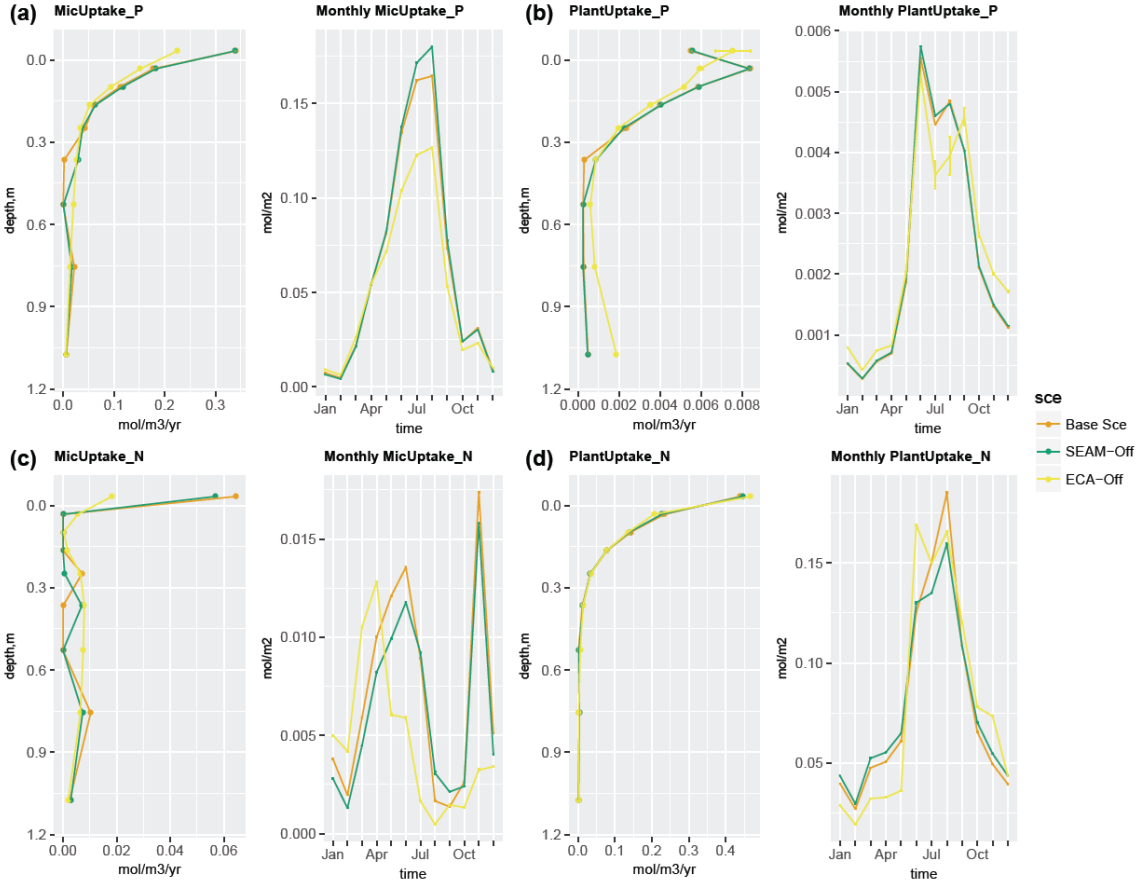

Figure 4. Simulated seasonal and vertical distribution of (a) microbial inorganic P uptake, (b) plant P uptake, (c) microbial inorganic N uptake, and (d) plant N uptake at the study site for the whole soil profile. Points represent the mean values and error bars represent the standard deviations, both calculated using data of the last 10 years from the model experiments.

https://doi.org/10.5194/gmd-2019-187
Preprint. Discussion started: 25 September 2019

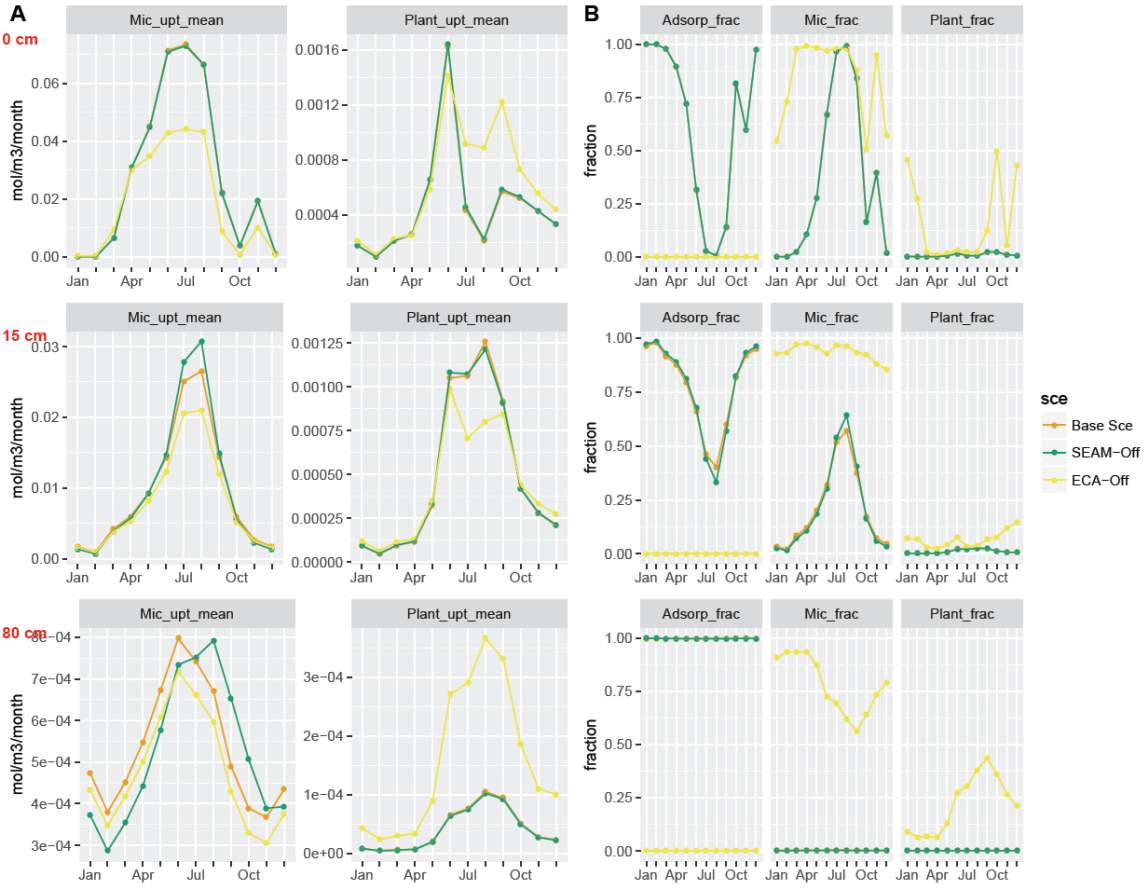

Figure 5. Simulated (A) microbial P uptake and plant P uptake rates and (B) relative competitiveness (in fractions) of P adsorption, microbial P uptake, and plant P uptake at 0cm depth (O-A horizon, upper panel), 15cm depth (A-B horizon , middle panel), and 80cm depth (B-C horizon, bottom panel). In panel (A), monthly mean values at different depths are presented through the whole year; in panel (B), relative competitiveness is calculated as the fraction of the individual rate to the sum of all three rates (P adsorption rate, microbial P uptake, and plant P uptake). All data points are derived from the last 10 years' data of the model experiments.

https://doi.org/10.5194/gmd-2019-187
Preprint. Discussion started: 25 September 2019

Geoscientific Model Development Discussions

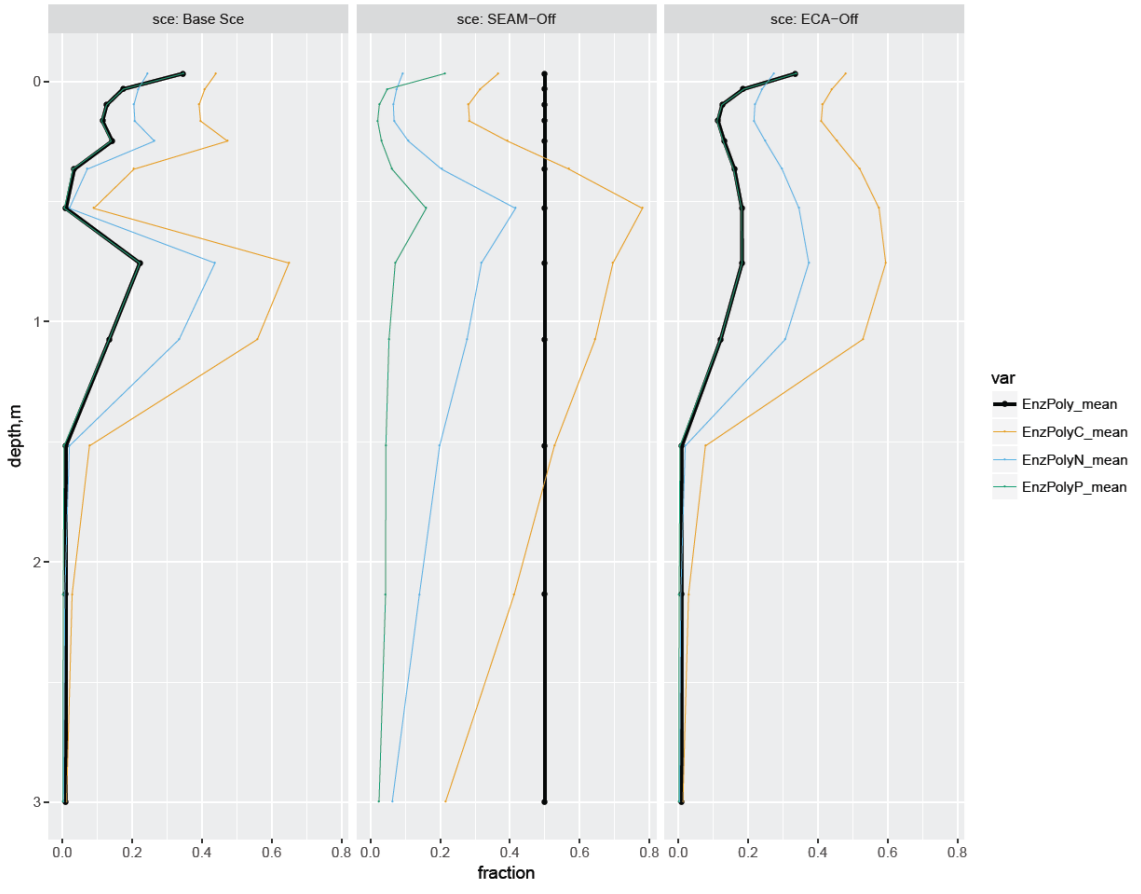

Figure 6. Simulated actual enzyme allocation to polymeric litter compared with potential enzyme allocations to polymeric litter given that element C/N/P is most limiting. Black lines: actual fraction of enzyme allocated to polymeric litter; orange/blue/green lines: potential enzyme allocation to polymeric litter to maximize C/N/P. Left panel: Base Scenario, middle panel: SEAM-Off scenario, right panel: ECA-Off scenario. All data points are derived from the last 10 years' data of the model experiments.

https://doi.org/10.5194/gmd-2019-187
Preprint. Discussion started: 25 September 2019

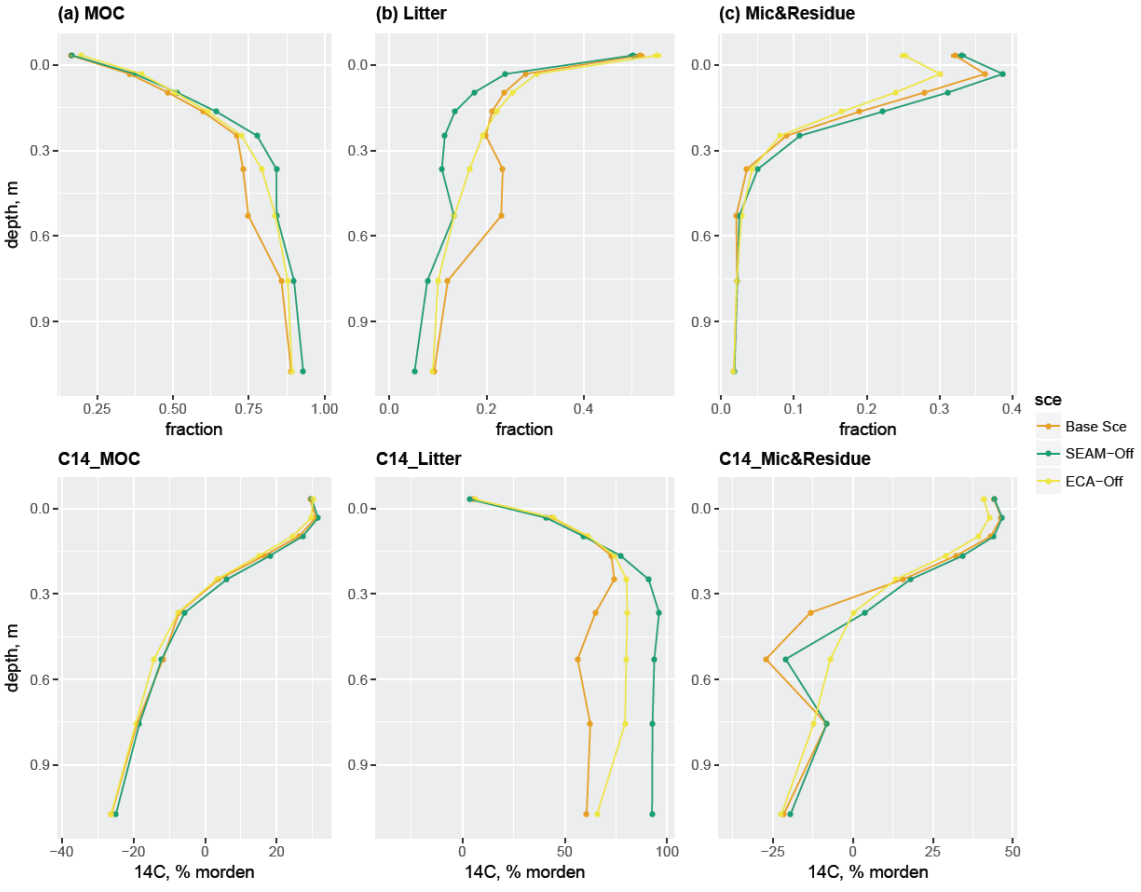

Figure 7. Simulated SOC fractions (upper panel) and their respective radiocarbon profiles (bottom panel) for up to 1m soil depth. Column (a): mineral-associated carbon (MOC), including adsorbed DOM and adsorbed microbial residue; Column (b): litter, including woody, polymeric and soluble litter; Column (c): live and dead microbes. Data points are derived from the last 10 years' data of the model experiments. All model experiments are only 200 years and not validated against the measured $\Delta^{14}C$.

https://doi.org/10.5194/gmd-2019-187
Preprint. Discussion started: 25 September 2019

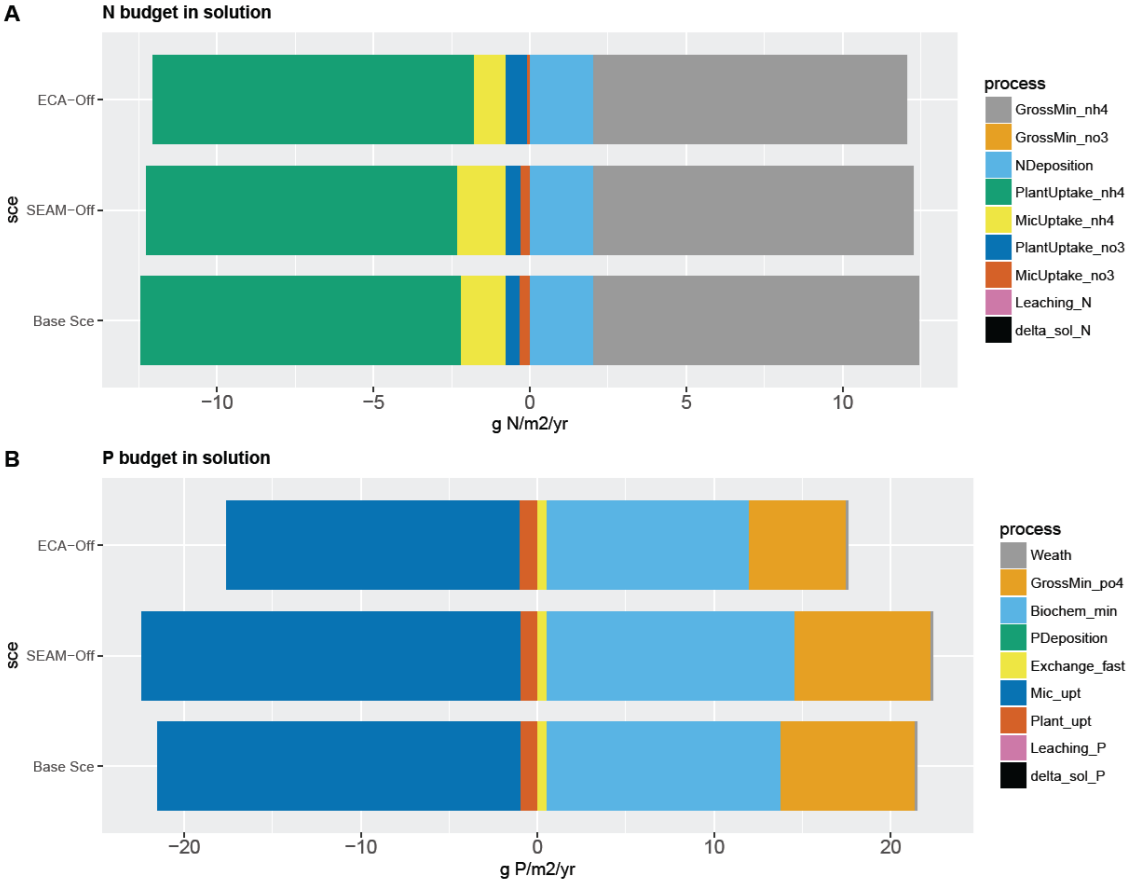

Figure 8. Simulated yearly budget of (A) nitrogen and (B) phosphorus in soil solution. In panel A, sourcing fluxes of N includes gross mineralisation of NH_4 and NO_3, N deposition; sinking fluxes of N includes plant and microbial uptake of NH_4, plant and microbial uptake of NO_3, N leaching (both inorganic and organic), and size change of soluble N ($delta\_sol\_N$). In panel B, sourcing fluxes of P includes weathering, gross mineralisation of PO_4, biochemical mineralisation of PO_4, P deposition; sinking fluxes of P includes adsorption ($Exchange\_fast$), microbial and plant uptake, P leaching (both inorganic and organic), and size change of soluble P ($delta\_sol\_P$). The budget are calculated using data of the full simulation (200 years) from the model experiments.

https://doi.org/10.5194/gmd-2019-187
Preprint. Discussion started: 25 September 2019

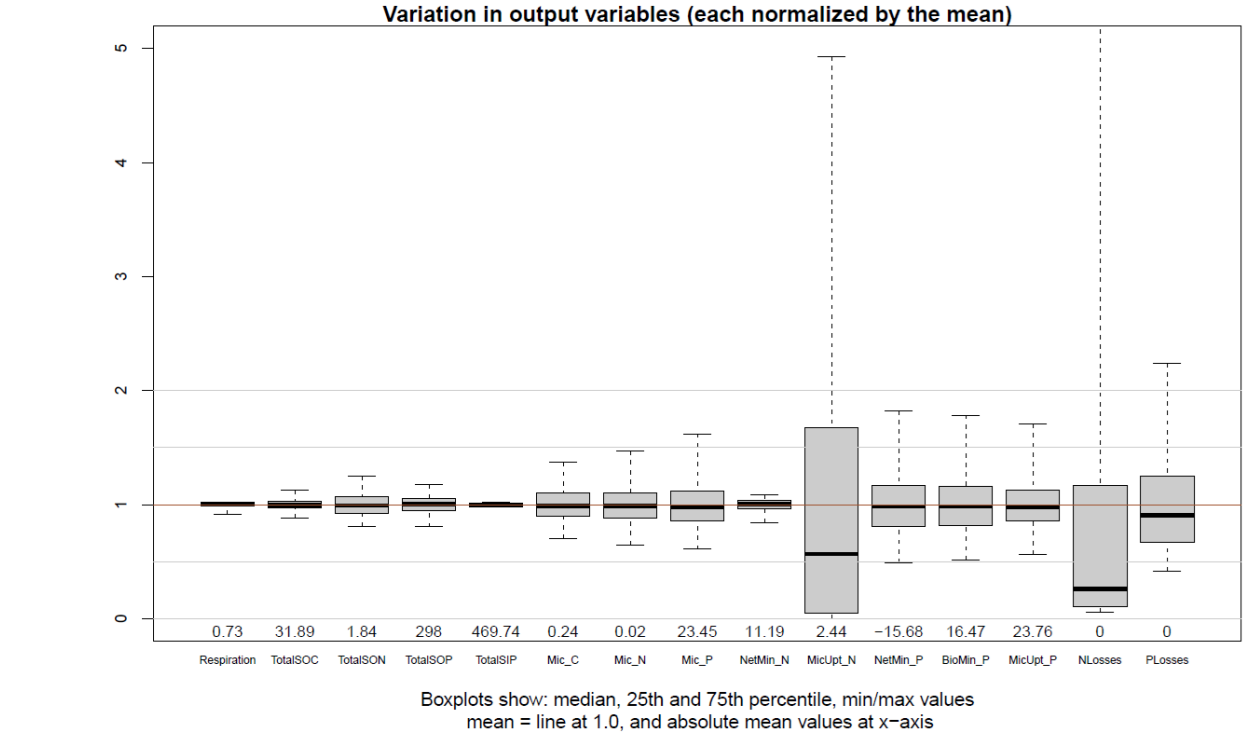

Figure 9. Normalized output variations in the LHS sensitivity analysis. The selected output variables include respiration, total soil organic C, N, and P, microbial C, N, and P, net N mineralisation, microbial N uptake, net P mineralisation, biomineralisation of P, microbial P uptake, the losses of N and P. All the calculations are done for the topmost one meter soil based on the data from the last 10 years of the 1000 LHS simulations.

https://doi.org/10.5194/gmd-2019-187
Preprint. Discussion started: 25 September 2019

Geoscientific Model Development Discussions
Open Access
EGU

Table 1. The annual soil C, N and P fluxes of model experiments at the study site. Positive values infer accumulation in the soil, and negative values infer loss from the soil. The values are the accumulated sum of the whole soil profile, calculated based on the data from the last 10 years of the model experiments.

Variable	Unit	Base Scenario	SEAM-Off	ECA-Off
Biogeochemical fluxes				
C litterfall	$\mathrm{gC\ m^{-2}\ yr}$	788.0	788.0	788.0
Respiration	$\mathrm{gC\ m^{-2}\ yr}$	-741.0	-746.2	-746.2
ΔSOC	$\mathrm{gC\ m^{-2}\ yr}$	47.0	41.8	41.8
N litterfall	$\mathrm{gN\ m^{-2}\ yr}$	14.52	14.52	14.52
N deposition	$\mathrm{gN\ m^{-2}\ yr}$	2.04	2.04	2.04
Plant N uptake	$\mathrm{gN\ m^{-2}\ yr}$	-13.29	-13.26	-13.28
N leaching	$\mathrm{gN\ m^{-2}\ yr}$	-0.01	-0.01	-0.01
ΔSON	$\mathrm{gN\ m^{-2}\ yr}$	3.25	3.29	3.26
P litterfall	$\mathrm{mgP\ m^{-2}\ yr}$	980.4	980.4	980.4
P deposition	$\mathrm{mgP\ m^{-2}\ yr}$	4.2	4.2	4.2
P weathering	$\mathrm{mgP\ m^{-2}\ yr}$	155.6	155.6	142.6
Plant P uptake	$\mathrm{mgP\ m^{-2}\ yr}$	-852.0	-866.8	-886.9
P leaching	$\mathrm{mgP\ m^{-2}\ yr}$	-0.3	-0.3	-1.7
P desorption	$\mathrm{mgP\ m^{-2}\ yr}$	-233.0	-243.8	-185.6
ΔSOP	$\mathrm{mgP\ m^{-2}\ yr}$	520.9	516.9	424.1

https://doi.org/10.5194/gmd-2019-187
Preprint. Discussion started: 25 September 2019

Geoscientific Model Development Discussions

Table 2. The five most important parameters (Par) and their respective RPCC for each output variable and the overall model importance (OVI). The RPCC is calculated for each output variable, and the overall importance of parameters is measured by calculating the mean of the absolute RPCC values across all output variables, weighted by the uncertainty contribution of these model outputs. The parameters are listed in Tab.S4 and explained in Tab.S3.

	Rank 1		**Rank 2**		**Rank 3**		**Rank 4**		**Rank 5**	
Variable	Par	RPCC	Par	RPCC	Par	RPCC	Par	RPCC	Par	RPCC
Total SOC	$v^{poly}_{max,depoly}$	-0.84	$v^{res}_{max,depoly}$	-0.80	$\frac{1}{\tau_{mic}}$	0.83	$\eta_{C,wl\rightarrow poly}$	0.71	$\eta_{C,sol\rightarrow dom}$	0.66
Total SON	$\chi^{C:N}_{mic}$	-0.99	$v^{res}_{max,depoly}$	-0.94	$\eta_{C,sol\rightarrow dom}$	0.84	$\chi^{N:P}_{mic}$	0.40	$\eta_{C,wl\rightarrow poly}$	0.38
Total SOP	$\chi^{C:N}_{mic}$	-0.97	$\chi^{N:P}_{mic}$	-0.97	$v_{max,biomin}$	-0.84	$\eta^{P}_{res\rightarrow dom}$	-0.78	$\frac{1}{\tau_{mic}}$	0.74
Total SIP	k_{weath}	-0.58	$\eta^{P}_{res\rightarrow dom}$	0.57	$v_{max,biomin}$	0.47	$\chi^{N:P}_{mic}$	0.45	$\eta^{P}_{res\rightarrow dom}$	-0.42
Microbial C	$\frac{1}{\tau_{mic}}$	-0.98	$\eta_{C,sol\rightarrow dom}$	0.86	$\chi^{C:N}_{mic}$	0.68	$\chi^{N:P}_{mic}$	0.67	$\eta_{C,wl\rightarrow poly}$	0.67
Microbial N	$\frac{1}{\tau_{mic}}$	-0.97	$\chi^{C:N}_{mic}$	-0.95	$\eta_{C,sol\rightarrow dom}$	0.83	$\chi^{N:P}_{mic}$	0.63	$\eta_{C,wl\rightarrow poly}$	0.62
Microbial P	$\frac{1}{\tau_{mic}}$	-0.96	$\chi^{N:P}_{mic}$	-0.94	$\chi^{C:N}_{mic}$	-0.93	$\eta_{C,sol\rightarrow dom}$	0.79	$\eta_{C,wl\rightarrow poly}$	0.55
Respiration	$\frac{1}{\tau_{mic}}$	-0.71	$\chi^{N:P}_{mic}$	0.69	$\chi^{C:N}_{mic}$	0.65	$v^{res}_{max,depoly}$	0.45	mic^{min}_{cue}	-0.37
Net N mineralisation	$\chi^{C:N}_{mic}$	0.97	$v^{res}_{max,depoly}$	0.65	mic^{min}_{cue}	-0.40	$\eta_{C,sol\rightarrow dom}$	-0.32	$\frac{1}{\tau_{mic}}$	-0.29
Microbial N uptake	mic_{nue}	-0.98	$\chi^{C:N}_{mic}$	-0.90	$\eta_{C,sol\rightarrow dom}$	0.75	$\eta_{C,wl\rightarrow poly}$	0.38	$\chi^{N:P}_{mic}$	0.21
Net P mineralisation	$\eta^{P}_{res\rightarrow dom}$	0.94	$\chi^{N:P}_{mic}$	0.84	$\chi^{C:N}_{mic}$	0.84	$\eta_{C,sol\rightarrow dom}$	-0.67	$\eta_{C,wl\rightarrow poly}$	-0.53
P Bio-mineralisation	$\eta^{P}_{res\rightarrow dom}$	-0.94	$\chi^{N:P}_{mic}$	-0.85	$\chi^{C:N}_{mic}$	-0.84	$\eta_{C,sol\rightarrow dom}$	0.67	$\eta_{C,wl\rightarrow poly}$	0.54
Microbial P uptake	mic_{pue}	-0.91	$\chi^{N:P}_{mic}$	-0.90	$\chi^{C:N}_{mic}$	-0.89	$\eta^{P}_{res\rightarrow dom}$	-0.85	$\eta_{C,sol\rightarrow dom}$	0.70
N Losses	$\chi^{N:P}_{mic}$	0.72	$\frac{1}{\tau_{mic}}$	-0.72	$\chi^{C:N}_{mic}$	0.67	$v^{dom}_{max,upt}$	0.41	$v_{max,biomin}$	0.35
P Losses	$v^{dom}_{max,upt}$	0.22	mic_{pue}	0.15	mic^{min}_{cue}	-0.14	$\eta^{P}_{res\rightarrow dom}$	-0.11	$k^{P}_{enz,mic}$	-0.55
OVI	$\chi^{C:N}_{mic}$	0.73	$\chi^{N:P}_{mic}$	0.57	$\frac{1}{\tau_{mic}}$	0.47	$\eta_{C,sol\rightarrow dom}$	0.42	$\eta^{P}_{res\rightarrow dom}$	0.35